Small-Conductance Ca^{2+}-Activated K^+ Channel Activation Deteriorates Hypoxic Ventricular Arrhythmias via CaMKII in Cardiac Hypertrophy

Taro Tenma[*1], Hirofumi Mitsuyama[*1], Masaya Watanabe[*1], Naoya Kakutani[*1], Yutaro Otsuka[*2], Kazuya Mizukami[*3], Rui Kamada[*1], Masayuki Takahashi[*1], Shingo Takada[*1], Hisataka Sabe[*2], Hiroyuki Tsutsui[*4], and Hisashi Yokoshiki[*1]

[*1] Department of Cardiovascular Medicine, Hokkaido University Graduate School of Medicine, Sapporo, Hokkaido, 060-8638, Japan
[*2] Department of Molecular Biology, Graduate School of Medicine, Hokkaido University, Sapporo, Hokkaido, 060-8638, Japan
[*3] Department of Cardiovascular Medicine, National Hospital Organization Hokkaido Medical Center, Sapporo, Hokkaido, 063-0005, Japan
[*4] Department of Cardiovascular Medicine, Kyusyu University Graduate School of Medicine, Fukuoka, Kyusyu, 812-8582, Japan

Running Head: SK channels deteriorate hypoxic ventricular arrhythmia

Correspondence:
Hisashi Yokoshiki MD, PhD
Department of Cardiovascular Medicine, Hokkaido University Graduate School of Medicine, Kita-15, Nishi-7, Kita-ku, Sapporo, Hokkaido 060-8638, Japan.
E-mail: yokoshh@med.hokudai.ac.jp

Abstracts

The molecular and electrophysiological mechanisms of acute ischemic ventricular arrhythmias in hypertrophied hearts are not well known. We hypothesized that small-conductance Ca^{2+}-activated K^+ (SK) channels are activated during hypoxia via the Ca^{2+} / calmodulin-dependent protein kinase II (CaMKII)-dependent pathway. We used normotensive Wistar-Kyoto (WKY) rats and spontaneous hypertensive rats (SHRs) as a model of cardiac hypertrophy. Inhibitory effects of SK channels and ATP-sensitive K^+ (K_{ATP}) channels on electrophysiological changes and genesis of arrhythmias during simulated global hypoxia (GH) were evaluated. Hypoxia-induced abbreviation of action potential duration (APD) occurred earlier in ventricles from SHRs vs. WKY rats. Apamin, a SK channel blocker, prevented this abbreviation in SHRs at both the early and delayed phase of GH, whereas in WKY rats only at the delayed phase. In contrast, SHRs were less sensitive to glibenclamide, a K_{ATP} channel blocker, which inhibited the APD abbreviation at both phase of GH in WKY rats. SK channel blockers (apamin and UCL-1684) reduced the incidence of hypoxia-induced sustained ventricular arrhythmias (SVAs) in SHRs, but not in WKY rats. Among three SK channel isoforms, SK2 channels were directly co-immunoprecipitated with phosphorylated CaMKII at Thr^{286} (p-CaMKII). We conclude that activation of SK channels leads to the APD abbreviation and SVAs during simulated hypoxia, especially in hypertrophied hearts. This mechanism may result from the p-CaMKII-bound SK2 channels and reveal new molecular targets to prevent lethal VAs during acute hypoxia in cardiac hypertrophy.

New and Noteworthy

We now show a new pathophysiological role of small-conductance Ca^{2+}-activated K^+ (SK) channels which shorten action potential duration and induce ventricular arrhythmias during hypoxia. We also demonstrate SK channels interacte with phosphorylated Ca^{2+} / calmodulin-dependent protein kinase II at Thr^{286} (p-CaMKII) in hypertrophied hearts.

Keywords

Small-conductance Ca^{2+}-activated K^+ (SK) channels; Myocardial hypoxia; Ventricular arrhythmia; Ca^{2+} / calmodulin-dependent protein kinase II (CaMKII); Cardiac hypertrophy.

Introduction

Acute myocardial ischemia induces arrhythmias and often leads to fatal outcomes (18, 27). The initial electrophysiological changes during acute myocardial ischemia include abbreviation of action potential duration (APD) and slowing of conduction velocity, which are related to accumulation of extracellular potassium ion (K^+) and increase in intracellular hydrogen ion due to products of anaerobic glycolysis. These changes appear to promote ischemia-induced ventricular arrhythmias (9, 47). Previous studies reported that left ventricular hypertrophy (LVH) had a higher incidence of ventricular fibrillation during acute hypoxia than normal hearts (22, 24). Besides, it was reported that the extent of shortening of APD caused by simulated hypoxia was greater in hypertrophied myocardium (22). However, its molecular and electrophysiological mechanisms have not been well elucidated.

Adenosine triphosphate (ATP)-sensitive K^+ (K_{ATP}) channels are weakly inward-rectifying K^+ channels that are activated by reduction of intracellular ATP concentration, thereby being operative during acute myocardial ischemia (3, 20, 47, 50). Thus, it is speculated that these channels play a significant role in the electrophysiological response to myocardial ischemia. On the other hand, K_{ATP} channel openers failed to alter extracellular K^+ accumulation during ischemia (19, 42). Moreover, using mice with knockout of Kir6.2 (a pore-forming subunit of cardiac K_{ATP} channel), it was demonstrated that activation of K_{ATP} channels were not the primary cause of extracellular K^+ accumulation during early myocardial ischemia (38). Indeed, we previously reported that activation of K_{ATP} channels under metabolic stress was impaired in rat hypertrophied left ventricular myocytes (39). Therefore, the mechanisms

other than K_{ATP} channels must also contribute to the extracellular K^+ accumulation during myocardial ischemia.

Small-conductance Ca^{2+} sensitive K^+ (SK) channels belong to a group of K^+ selective and voltage-independent ion channels which are inhibited by the bee toxin apamin (1, 2). These channels have a high Ca^{2+} sensitivity and are expressed in various tissues including heart (1). Chua et al from the Chen P-S's laboratory and we reported that apamin-sensitive SK channel currents played a significant role in action potential configurations in ventricular myocytes from failing rabbit and hypertrophied rat hearts (7, 30). We also demonstrated that SK channels were upregulated via the enhanced activation of Ca^{2+} / calmodulin-dependent protein kinase II (CaMKII) in hypertensive cardiac hypertrophy (29, 30).

In the present study, we hypothesized that the CaMKII activity during acute hypoxia could regulate the SK channel opening, which is prompted earlier in cardiac hypertrophy because of the higher basal activity of CaMKII. The earlier activation of SK channels would lead to enhanced shortening of APD, thereby being susceptible to sustained ventricular arrhythmias (SVAs) especially in hypertrophied hearts.

Materials and Methods

Ethical Approval

The research protocol was conformed to animal care guidelines for the Care and Use of Laboratory Animals in Hokkaido University Graduate School of Medicine, and was approved by our institutional animal research committee.

Materials

All experiments were executed using male 18 to 22-week-old Wistar-Kyoto (WKY) rats as control, and spontaneous hypertensive rats (SHRs) as a model of cardiac hypertrophy. SHRs at these ages are known to have established cardiac hypertrophy without any systolic dysfunction or heart failure (4, 32).

Surgical preparation

All animals were anesthetized with inhalation of diethyl ether (Nacalai tesque, Kyoto, Japan) and with intraperitoneal injection of the mixture which was made from medetomidine hydrochloride (0.15 mg/kg; Kyoritsu Seiyaku, Tokyo, Japan), midazolam (2 mg/kg; Astellas Pharma, Tokyo, Japan) and butorphanol (2.5 mg/kg; Meiji Seika Pharma, Tokyo, Japan). Under the full anesthesia, an intraperitoneal injection of heparin sodium (400 IU/kg) was performed. The excised heart was mounted on a Langendorff apparatus and retrogradely perfused with Tyrode solution (37 °C) containing (in mM) 143 NaCl, 5.4 KCl, 0.33 NaH_2PO_4, 5 HEPES, 5.5 glucose, 0.5 $MgCl_2$, and 1.8 $CaCl_2$ (pH 7.4 adjusted using NaOH) and gassed with 100% O_2 until the beating rate became stable. The perfusion pressure was kept at 70 cmH_2O for WKY rats and 100 cmH_2O for SHRs to adjust coronary flow per weight as described previously (23).

Simulated myocardial global hypoxia

The hearts were perfused until disappearance of premature contractions, for about 5 minutes. At this point, the heart rate was usually more than 200 beats / min. Then, the Langendorff-perfused hearts were switched to hypoxia / zero glucose solution (Tyrode solution gassed with 100% N_2 and containing no glucose) to make the simulated global hypoxia (GH) (22). Because GH induced bradycardia within a few minutes, the hearts were constantly paced from the apex of left ventricle (LV) at a cycle length of 300 ms.

Optical mapping

An optical mapping system was used to measure action potentials as previously described (29, 30, 45). The detail of optical mapping protocol was depicted in **Figure 1A**. A silver unipolar pacing electrode was attached to the apex of left ventricle (LV), and two electrodes were attached to LV and right ventricle (RV) to record the electrocardiogram (ECG). After the beating rate became stable, the perfusate was switched to Tyrode solution containing di-4-ANEPPS (2.5 μM, Life technologies, OR, USA) for 10 min. The heart was paced at a cycle length of 300 ms because heart rate decreased under di-4-ANEPSS perfusion (33). Then it was perfused with Tyrode solution containing blebbistatin (10 μM, TRC, Toronto, Canada), an excitation-contraction uncoupler without any effects on electrical parameters, to eliminate motion artifacts for 15 min (13). Illumination of the voltage sensitive dye's fluorescence was provided using a 531 ± 20-nm light emitted by a 150-W halogen light source. The fluorescence was filtered with a 590-nm interference bandpass filter and

acquired with charge-coupled device camera (MiCAM02, BrainVision, Tokyo, Japan) at 0.2-mm spatial (88 × 60 pixels) and 2.2-ms temporal resolutions. We performed optical mappings of anterior epicardial surface of LV at the pacing cycle length (PCL) of 300 ms from the apex of LV at twice the diastolic threshold currents with a silver unipolar electrode. Drugs were perfused from 15 minutes before stimulated hypoxia. We recorded optical membrane potentials at baseline, GH 15 min, and GH 30 min.

Digital filtering was routinely applied to improve signal-noise ratio of the optical data (25). We used the thresholding method (cut-off value was 25% of the maximal) for data masking. The 3 × 3 spatial and cubic filters were used to minimize the post-acquisition high-frequency noise. The components of the dominant-frequencies between 100 Hz and 250 Hz obtained by the Fourier transform were also removed. After the digital filtering, the APD of all available pixels on LV was measured at 90% repolarization (APD_{90}). On the other hand, signals from atrial area and pixels with inadequate action potentials at the edge of LV were excluded for the analysis. We defined the median APD_{90}, not mean APD_{90}, of all available pixels as the individual APD_{90} because its histograms were non-normal distribution. We determined the delta APD_{90} (ΔAPD_{90}) as a difference between the median APD_{90} at the baseline and that at the GH 15 min or GH 30 min. The APD_{90} maps for epicardial surface of LV were constructed by BV_ana software (version 1604, BrainVision).

Susceptibility to sustained ventricular arrhythmias

We recorded ECGs during GH to reveal the susceptibility to sustained ventricular arrhythmias (SVAs). ECGs of the Langendorff-perfused hearts were recorded with widely spaced unipolar electrodes on RV and LV using the PowerLab

4/26 (AD Instruments, Dunedin, New Zeeland). A unipolar electrode was also attached to LV apex for pacing. The hearts were initially perfused with oxygenated Tyrode solution (37°C) until beating of the hearts was stabilized. After that, they were subjected to the acute simulated GH protocol (**Figure 1B**). They were paced at the cycle length of 300 ms with twice the diastolic threshold currents during simulated GH. The stimulator output was raised in case the hearts exhibited the loss of capture. We evaluated the incidence of spontaneous ventricular arrhythmia during 30 minutes of simulated GH, not using rapid or extrastimulus pacing. The pacing was stopped as soon as spontaneous SVAs occurred. No arrhythmia was induced by the stimulation on a T-wave. We defined a spontaneous rapid ventricular arrhythmia as a SVA when it lasted more than 10 seconds. To examine the effects of drugs on hypoxia-induced SVAs, we applied simulated GH for 30 min to the Langendorff-perfused hearts in the absence or presence of drugs.

Western Blot

LV tissues were snap frozen, and homogenized on ice in cell lysis buffer (Cell Signaling Technology, MA, USA) supplemented with Complete Protease Inhibitor Cocktail (Roche, Basel, Switzerland). After centrifugation, the supernatants were collected and stored at -80°C until the time of assay. The protein concentration was quantified by the BCA Protein Assay (ThermoFisher Scientific, MA, USA). The proteins were then electrophoretically separated on SDS-PAGE in the Western running buffer (70 mM Tris, 192 mM glycine, 0.1% SDS, and 20% methanol, pH 8.3), transferred onto polyvinylidene difluoride (PVDF) membranes, and blocked with 5% nonfat dry milk or 5% BSA. The membranes were incubated with antibodies against

target antigens, that is, anti-SK1, anti-SK2, anti-SK3 (1:200 dilution), anti-Kir6.2 (1:200 dilution), and anti-p-CaMKII (Thr^{286}, 1:1000 dilution) for overnight at 4°C. Horseradish peroxidase-conjugated secondary antibodies were used for the secondary detection (1:5000 dilution). Bands were detected with ChemiDoc XRS+ (Bio-Rad, CA, USA) on ECL or ECL Prime Reagent (GE, Chicago, USA). The intensity of bands was quantified using ImageJ software (National Institutes of Health, USA). GAPDH (1:5000 dilution) was used as an internal control for the intensity of detected bands in each lane.

Immunoprecipitation

The lysates of LV tissue sample were centrifuged, and the supernatant fluid was collected. The lysates were mixed with an anti-p-CaMKII (Thr^{286}), anti-SK1, anti-SK2, anti-SK3 and normal rabbit IgG as a control, and incubated overnight at 4°C. After the addition of protein-A (rProtein A Sepharose Fast Flow, GE), the lysates were incubated for 2 h at 4°C. Protein-A was washed with buffer (150 mM NaCl, 50 mM Tris-HCl, 0.5% Triton-X) for 5 times and then mixed with 2× SDS sample buffer with boiling for 5 min at 95°C. Western blot with anti-SK1, anti-SK2, and anti-SK3 for the proteins of labeled anti-p-CaMKII (Thr^{286}), and with anti-p-CaMKII (Thr^{286}) for the proteins of labeled anti-SK1, anti-SK2, and anti-SK3 was performed as described above. Horseradish peroxidase-conjugated secondary antibodies (TrueBlot®; 1:1000 dilution) were used for the secondary detection.

Drugs

Apamin (100 nM, PEPTIDE, Osaka, Japan) and UCL-1684 (1 μM, Tocris, Bristol, UK) which inhibit the activity of SK channels, and glibenclamide (10 μM,

Wako, Osaka, Japan), an K_{ATP} channel blocker, were added to Tyrode solution and perfused for 15 min before and during GH.

Antibodies

All primary antibodies were purchased from commercial sources as follows: rabbit polyclonal antibodies against SK1 (Alomone labs, Jerusalem, Israel), SK2 (Alomone labs), SK3 (Alomone labs), Kir6.2 (Alomone labs); and mouse monoclonal antibodies against Thr286-phospholylated CaMKII (Abcam, Cambridge, UK); GAPDH, which conjugated secondary antibodies (Cell Signaling Technology). Secondary antibodies for western blot and immunoprecipitation were from Santa Cruz Biotechnology, CA, USA and Rockland Immunochemicals, PA, USA, respectively.

Data analyses

All data are expressed as means ± SE. Statistical differences of the means between two independent groups were determined using a Student's *t*-test. For multiple group comparisons, one-way or two-way ANOVA were performed when appropriate. For the post hoc test in the ANOVA, a Sidak's or Tukey's multiple-comparison test was performed. Categorical data were compared with Fisher's exact test. Survival distributions were calculated using Kaplan-Meier curves and the log-rank *P* values were adjusted with holm's method. Differences with *P* values of < 0.05 were considered to be significant.

Results

Animal Characteristics

We confirmed that SHRs used in the present study had ventricular hypertrophy (heart weight / body weight: 4.44 ± 0.09 mg/g in WKY rats vs. 5.53 ± 0.07 mg/g in SHRs, $P < 0.0001$).

Susceptibility to APD abbreviation and SVAs during simulated hypoxia in hypertrophied hearts

As with previous report (23), the APD_{90} in SHRs were longer than that in WKY rats at the baseline and any time during the GH (WKY rats vs. SHRs, $P < 0.001$, **Figure 2A**). And, in both WKY rats and SHRs, APD_{90} at PCL of 300 ms shortened time-dependently during simulated GH. However, the hypoxia-induced abbreviation of APD_{90} in SHRs occurred earlier as compared with that in WKY rats: significant APD_{90} abbreviation from baseline (state of no GH) occurred at GH 20 min in WKY rats, and it did at GH 10 min in SHRs (**Figure 2A**). Similarly, the onset-time of SVAs was earlier in SHRs than in WKY rats (22.9 ± 0.9 min in WKY rats vs. 10.9 ± 0.5 min in SHRs, $P < 0.01$, **Figure 2B**). The percentage of hearts developing SVAs during GH was higher in SHRs than in WKY rats (22% in WKY rats vs. 100% in SHRs at GH 15 min, log-rank $P < 0.01$, **Figure 2C**).

Electrophysiological and molecular changes during simulated hypoxia in normal hearts (WKY)

To evaluate the involvement of activation of SK channels and K_{ATP} channels in

the hypoxia-induced APD_{90} abbreviation, we performed the optical mapping study using apamin (100 nM), a SK channel blocker and glibenclamide (10 μM), a K_{ATP} channel blocker. **Figures 3A and 3B** show representative optical action potentials and the APD_{90} map of LV in WKY rats during simulated GH. The APD_{90} at the PCL of 300 ms shortened time-dependently during simulated GH in the control condition. At the early phase of hypoxia (at GH 15 min), pretreatment with apamin did not prevent the hypoxia-induced APD_{90} abbreviation, however, that with glibenclamide significantly reduced it (ΔAPD at GH 15 min: -6.67 ± 0.53 ms [control: CON], -5.70 ± 1.62 ms [apamin: APA], -1.50 ± 1.70 ms [glibenclamide: GLB]; CON vs. APA, $P = 0.82$; CON vs. GLB, $P = 0.03$) (**Figure 3C**). On the other hand, at the delayed phase of hypoxia (at GH 30 min), not only glibenclamide but also apamin prevented the hypoxia-induced APD_{90} abbreviation (ΔAPD at GH 30 min: -15.00 ± 0.87 ms [CON], -6.88 ± 1.70 ms [APA], -4.50 ± 3.39 ms [GLB]; CON vs. APA, $P = 0.04$; CON vs. GLB, $P = 0.02$) (**Figure 3C**). We recorded ECGs continuously during simulated GH and evaluated the incidence of spontaneous SVAs. Representative ECG traces during simulated GH in the absence of drugs (control) and the presence of apamin were depicted in **Figures 3D**, respectively. Neither SK channel blockers (apamin, UCL-1684) nor K_{ATP} channel blocker (glibenclamide) prevented the hypoxia-induced SVAs, effectively (**Figures 3E**). The amount of protein expression of three isoforms of SK channels and Kir6.2 (which is a pore-forming subunit of the K_{ATP} channel) in left ventricular myocardium did not change during simulated GH (**Figures 3F and 3G**).

Electrophysiological and molecular changes during simulated hypoxia in hypertrophied hearts (SHR)

We also performed the optical mapping study in SHRs. The representative optical action potentials and the APD_{90} map of LV during simulated GH were depicted in **Figures 4A and 4B**. The APD_{90} of LV at the PCL of 300 ms shortened time-dependently during simulated GH in the control condition. In both the early and delayed phase of hypoxia, pretreatment with apamin, but not with glibenclamide, dramatically prevented the hypoxia-induced APD_{90} abbreviation (ΔAPD at GH 15 min: -13.33 ± 3.63 ms [CON], -0.5 ± 1.22 ms [APA], -5.59 ± 1.83 ms [GLB]; CON vs. APA, $P = 0.03$; CON vs. GLB, $P = 0.24$), (ΔAPD at GH 30 min: -27.5 ± 5.95 ms [CON], -3.0 ± 2.00 ms [APA], -16.01 ± 3.69 ms [GLB]; CON vs. APA, $P = 0.02$; CON vs. GLB, $P = 0.38$) (**Figure 4C**). We also examined the vulnerability to hypoxic SVAs in SHRs. **Figures 4D** demonstrated the representative ECG traces during simulated GH in control and in the presence of apamin, respectively. **Figure 4E** showed Kaplan-Meier curves of the event-free survival for spontaneous SVAs during simulated GH. Notably, SK channel blockers (apamin, UCL-1684) significantly prevented the hypoxia-induced SVAs (**Figures 4E**). However, the expression level of isoforms of SK channels and Kir6.2 in left ventricular myocardium were unchanged during simulated GH (**Figures 4F and 4G**).

Spatial heterogeneity of repolarization during simulated hypoxia

The coefficient of variation of APD_{90} was calculated from action potentials of all available points during control, GH 15 min, and 30 min in WKY rats (**Figure 5A**) and SHRs (**Figure 5B**). There were no significant differences of the coefficient of variation among three groups at any hypoxia stage in both WKY rats and SHRs (**Figure 5**). In other words, no drugs (not only glibenclamide but also apamin) could reduce the

spatial heterogeneity of repolarization as assessed by the coefficient of variation of APD_{90}.

Molecular Differences of Left Ventricles between WKY rats and SHRs

The amount of phosphorylated CaMKII at Thr^{286} (p-CaMKII) from SHRs was higher than that from WKY rats at the baseline (**Figure 6A**). During the simulated GH, the expression level of p-CaMKII increased time-dependently in WKY rats, whereas that in SHRs was unchanged (**Figure 6B**). At the baseline, among three isoforms, the expression of SK2 channel was higher in SHRs as compared with WKY rats (**Figure 6C**). With regard to Kir6.2, there was no significant difference between WKY rats and SHRs at the baseline (**Figure 6D**).

Interaction of SK channels and p-CaMKII in Left Ventricular Myocardium

Based on the above findings, we thought that p-CaMKII played a major role in SK channel activation. Therefore, we performed immunoprecipitation to identify the interaction of p-CaMKII and SK channels from SHRs. As shown in **Figure 7A**, anti-p-CaMKII antibodies co-immunoprecipitated only SK2 channel protein. Consistent with this observation, only anti-SK2 antibodies co-immunoprecipitated p-CaMKII (**Figure 7B**).

Discussions

We demonstrated three major findings in the present study. Simulated myocardial hypoxia activated SK channel currents, which contributed to the APD abbreviation and ventricular arrhythmias specifically during the early phase (i.e., within 15 min of hypoxia) in hypertrophied hearts from SHRs. Increase in the CaMKII activity assessed by the amount of p-CaMKII was correlated to activation of SK channels during hypoxia in normal ventricles from WKY rats. SK channel upregulation appeared to be mediated through the binding of p-CaMKII to SK2 channels.

SK Channel Upregulation in the Diseased Hearts and Pathophysiological Conditions

A previous report showed that apamin did not change action potential configurations in rat and human normal ventricles under physiological conditions, although SK channels were expressed in ventricular myocardium (31). However, in the diseased animal models such as heart failure, acute and chronic myocardial infarction, and cardiac hypertrophy, apamin-sensitive K^+ currents, that is, presumable SK channel currents, were present and / or contributed to action potential configurations (7, 15, 26, 30). Moreover, hypokalemia activated SK channel currents in normal rabbit ventricles without heart failure (5). Interestingly, previous studies reported that the pathophysiological conditions including cardiac hypertrophy, heart failure and hypokalemia activated CaMKII (14, 21, 29, 30, 35, 51). In the present study, we demonstrated that CaMKII was time-dependently activated during the simulated acute hypoxia, which coincided with the apamin-inhibitory APD abbreviation in normal

ventricular myocardium (i.e., hearts from WKY rats) (**Figures 3A, 3B, 3C and Figure 6B**). Therefore, we consider that SK channel activation is closely associated with the CaMKII activity.

CaMKII Activation during Acute Myocardial Ischemia

Activation of CaMKII during acute ischemia has been reported in neurons (44). However, there were only a few studies which examined the CaMKII activity in acute myocardial ischemia (41, 43). Uemura et al reported that myocardial ischemia reduced autophosphorylation of CaMKII (41). In another study using Langendorff-perfused rat hearts, phosphorylation of phospholamban Thr^{17} by CaMKII, which reflected the CaMKII activity, transiently increased at 2 - 5 minutes of ischemia, but declined to the preischemic value at 10 minutes (43). In these studies, myocardial ischemia was produced by interruption of the coronary flow, resulting in termination of the heart beating. This phenomenon might influence the CaMKII activity because of its rate-dependency (8, 49), therefore, we applied the simulated hypoxic condition to Langendorff-perfused hearts with a perfusate of the hypoxia / zero glucose Tyrode solution during ventricular pacing at a cycle length of 300 ms. In our experiments, acute myocardial hypoxia increased p-CaMKII in normal ventricular myocardium from WKY rats. In contrast, the level of p-CaMKII remained unchanged during acute hypoxia in hypertrophied ventricular myocardium from SHRs (**Figure 6B**). This might be because the CaMKII activity was already too high at the baseline to be stimulated during acute myocardial hypoxia in cardiac hypertrophy.

Phosphorylated CaMKII at Thr^{286} (p-CaMKII) Binding to SK Channels

Previous studies showed the direct interaction between CaMKII and potassium channel subunits: Kv1.4 and Kir6.2 (37, 40). These subunits form transient outward currents (Ito) and the cardiac K_{ATP} channel currents (50), respectively. The present study found a novel interaction between p-CaMKII and SK2 channels. Since (a) the affinity of CaMKII for calmodulin (CaM) increases 1000 times after autophosphorylation (that is, p-CaMKII) (28) and (b) SK channels have the CaM-binding domain (48), it would be possible that p-CaMKII interacts with SK channels through CaM. This interaction might change the Ca^{2+} sensitivity of SK channels, thereby resulting in the different time-course of SK channel activation during acute myocardial hypoxia between normal hearts (WKY rats) and hypertrophied hearts (SHRs) (**Figure 8**).

SK Channels as Arrhythmogenic Substrate

Previous studies reported that SK channels in atrial and pulmonary vein myocytes were upregulated by atrial tachycardia pacing (34, 36) and that inhibition of SK channels terminated and protected against atrial fibrillation (10, 11, 16). Regarding ventricular arrhythmias, inhibition of SK currents by apamin prevented an excessive shortening of APD and recurrent ventricular fibrillation (VF) immediately after electrical shocks in failing rabbit ventricles (7). In contrast, in a rabbit model of tachycardia-induced heart failure with complete atrio-ventricular block, apamin prolonged the QT interval, and in some cases, induced a torsade de pointes like polymorphic VT (6). In another study, apamin prolonged APD at long and short, but not at intermediate pacing cycle length in failing ventricles. As a result, a slope of APD restitution curve was reduced by apamin in failing hearts (17). Taken together, SK channel upregulation in heart failure may be antiarrhythmic by preserving the

repolarization reserve at slow heart rate, but could be proarrhythmic by steepening the slope of APD restitution curve, which promotes generation and maintenance of VF. In the present study, apamin prevented APD_{90} abbreviation during global hypoxia especially in hypertrophied ventricles (**Figure 4C**). On the other hand, spatial heterogeneity of repolarization, which was evaluated as the coefficient of variation of APD_{90} (**Figure 5**), was not reduced by apamin. In addition, it has not been demonstrated that hypoxic activation of SK channels produces the steepness of APD restitution. Therefore, the arrhythmogenic mechanism of SK channel activation during hypoxia remains to be determined.

Using a rat model of acute regional infarction that was produced by ligation of the left anterior descending coronary artery, Gui et al reported the preventive effect of SK channel blockers, apamin and UCL-1684, on ischemia-induced ventricular arrhythmias. In addition, a shortening of monophasic APD in ischemic area was alleviated by SK channel blockers (15). In our study, hypoxia / zero glucose solution was used as the simulated hypoxic condition, and we found a significant inhibition of SVAs by SK channel blockers only in hypertrophied hearts (SHRs) (**Figures 3E and 4E**). However, we also observed that the APD abbreviation after 30 minutes GH was partially prevented by apamin in normal hearts (WKY rats) (**Figures 3A, 3B, and 3C**). Therefore, different experimental conditions may explain some discrepancy between our study and a previous one (15). Further studies are necessary to address the functional roles of SK channels in ventricular arrhythmias especially under the pathophysiological conditions.

Study Limitation

We used SHR as a model of cardiac hypertrophy. SHR is known as a genetic model of hypertension and has been commonly used as an animal model of hypertrophy (12). The results in the present study may need further validation in other models of cardiac hypertrophy. We used the hypoxia / zero glucose Tyrode solution to prepare simulated GH. We should have stopped the coronary perfusion with Tyrode solution to make actual GH. However, we chose the former to acquire the electrophysiological data during simulated hypoxia, in which the heart can be paced. SK channels are present in the vascular endothelium and smooth muscle cells of the heart. The cell physiology of these channels provides hyperpolarizing K^+ currents that limit the Ca^{2+} influx, thereby regulating the tonic vascular tone (2, 46). Therefore, the observations in this study might be affected by the presence of SK channels in vascular cells. In the optical mapping study, the incidence of spontaneous hypoxic arrhythmias was very low even in SHRs and we failed to record the onset of these arrhythmias. The mechanism of ventricular arrhythmias induced by global hypoxia / ischemia remains to be elucidated.

Acknowledgements

We thank Noriko Ikeda, Yuki Kimura, and Miwako Yamane for technical assistance in our experiments.

Grants

This work was supported, in part, by Japan Society for the Promotion of Science Grant-in-Aid for Scientific Research 23591075 (to H. Yokoshiki).

Disclosures

No conflicts of interest, financial or otherwise, are declared by the author(s) in this study.

References

1. **Adelman JP, Maylie J, and Sah P**. Small-conductance Ca2+-activated K+ channels: form and function. *Annu Rev Physiol* 74: 245-269, 2012.

2. **Berkefeld H, Fakler B, and Schulte U**. Ca2+-activated K+ channels: from protein complexes to function. *Physiol Rev* 90: 1437-1459, 2010.

3. **Billman GE**. Role of ATP sensitive potassium channel in extracellular potassium accumulation and cardiac arrhythmias during myocardial ischaemia. *Cardiovasc Res* 28: 762-769, 1994.

4. **Chan V, Fenning A, Levick SP, Loch D, Chunduri P, Iyer A, Teo YL, Hoey A, Wilson K, Burstow D, and Brown L**. Cardiovascular changes during maturation and ageing in male and female spontaneously hypertensive rats. *J Cardiovasc Pharmacol* 57: 469-478, 2011.

5. **Chan YH, Tsai WC, Ko JS, Yin D, Chang PC, Rubart M, Weiss JN, Everett THt, Lin SF, and Chen PS**. Small-Conductance Calcium-Activated Potassium Current Is Activated During Hypokalemia and Masks Short-Term Cardiac Memory Induced by Ventricular Pacing. *Circulation* 132: 1377-1386, 2015.

6. **Chang PC, Hsieh YC, Hsueh CH, Weiss JN, Lin SF, and Chen PS**. Apamin induces early afterdepolarizations and torsades de pointes ventricular arrhythmia from failing rabbit ventricles exhibiting secondary rises in intracellular calcium. *Heart rhythm* 10: 1516-1524, 2013.

7. **Chua SK, Chang PC, Maruyama M, Turker I, Shinohara T, Shen MJ, Chen Z, Shen C, Rubart-von der Lohe M, Lopshire JC, Ogawa M, Weiss JN, Lin SF, Ai T, and Chen PS**. Small-conductance calcium-activated potassium channel and recurrent ventricular fibrillation in failing rabbit ventricles. *Circ Res* 108: 971-979, 2011.

8. **De Koninck P, and Schulman H**. Sensitivity of CaM kinase II to the frequency of Ca2+ oscillations. *Science* 279: 227-230, 1998.

9. **Di Diego JM, and Antzelevitch C**. Ischemic ventricular arrhythmias: experimental models and their clinical relevance. *Heart Rhythm* 8: 1963-1968, 2011.

10. **Diness JG, Skibsbye L, Jespersen T, Bartels ED, Sorensen US, Hansen RS, and Grunnet M**. Effects on atrial fibrillation in aged hypertensive rats by Ca(2+)-activated K(+) channel inhibition. *Hypertension* 57: 1129-1135, 2011.

11. **Diness JG, Sorensen US, Nissen JD, Al-Shahib B, Jespersen T, Grunnet M, and Hansen RS**. Inhibition of small-conductance Ca2+-activated K+ channels terminates and protects against atrial fibrillation. *Circ Arrhythm Electrophysiol* 3: 380-390, 2010.

12. **Doggrell SA, and Brown L**. Rat models of hypertension, cardiac hypertrophy and failure. *Cardiovasc Res* 39: 89-105, 1998.

13. **Fedorov VV, Lozinsky IT, Sosunov EA, Anyukhovsky EP, Rosen MR, Balke CW, and Efimov IR**. Application of blebbistatin as an excitation-contraction uncoupler for electrophysiologic study of rat and rabbit hearts. *Heart Rhythm* 4: 619-626, 2007.

14. **Ferreira JC, Moreira JB, Campos JC, Pereira MG, Mattos KC, Coelho MA, and Brum PC**. Angiotensin receptor blockade improves the net balance of cardiac Ca(2+) handling-related proteins in sympathetic hyperactivity-induced heart failure. *Life Sci* 88: 578-585, 2011.

15. **Gui L, Bao Z, Jia Y, Qin X, Cheng ZJ, Zhu J, and Chen QH**. Ventricular tachyarrhythmias in rats with acute myocardial infarction involves activation of small-conductance Ca2+-activated K+ channels. *Am J Physiol Heart Circ Physiol* 304: H118-130, 2013.

16. **Haugaard MM, Hesselkilde EZ, Pehrson S, Carstensen H, Flethoj M, Praestegaard KF, Sorensen US, Diness JG, Grunnet M, Buhl R, and Jespersen T**. Pharmacologic inhibition of small-conductance calcium-activated potassium (SK) channels by NS8593 reveals atrial antiarrhythmic potential in horses. *Heart rhythm* 12: 825-835, 2015.

17. **Hsieh YC, Chang PC, Hsueh CH, Lee YS, Shen C, Weiss JN, Chen Z, Ai T, Lin SF, and Chen PS**. Apamin-sensitive potassium current modulates action potential duration restitution and arrhythmogenesis of failing rabbit ventricles. *Circ Arrhythm Electrophysiol* 6: 410-418, 2013.

18. **Huikuri HV, Castellanos A, and Myerburg RJ**. Sudden death due to cardiac arrhythmias. *N Engl J Med* 345: 1473-1482, 2001.

19. **Kanda A, Watanabe I, Williams ML, Engle CL, Li S, Koch GG, and Gettes LS**. Unanticipated lessening of the rise in extracellular potassium during ischemia by pinacidil. *Circulation* 95: 1937-1944, 1997.

20. **Kantor PF, Coetzee WA, Carmeliet EE, Dennis SC, and Opie LH**. Reduction of ischemic K+ loss and arrhythmias in rat hearts. Effect of glibenclamide, a sulfonylurea. *Circ Res* 66: 478-485, 1990.

21. **Kirchhefer U, Schmitz W, Scholz H, and Neumann J**. Activity of cAMP-dependent protein kinase and Ca2+/calmodulin-dependent protein kinase in failing and nonfailing human hearts. *Cardiovasc Res* 42: 254-261, 1999.

22. **Kohya T, Kimura S, Myerburg RJ, and Bassett AL**. Susceptibility of hypertrophied rat hearts to ventricular fibrillation during acute ischemia. *J Mol Cell Cardiol* 20: 159-168, 1988.

23. **Kohya T, Yokoshiki H, Tohse N, Kanno M, Nakaya H, Saito H, and Kitabatake A**. Regression of left ventricular hypertrophy prevents ischemia-induced lethal arrhythmias. Beneficial effect of angiotensin II blockade. *Circ Res* 76: 892-899, 1995.

24. **Koyanagi S, Eastham C, and Marcus ML**. Effects of chronic hypertension and left ventricular hypertrophy on the incidence of sudden cardiac death after coronary artery occlusion in conscious dogs. *Circulation* 65: 1192-1197, 1982.

25. **Laughner JI, Ng FS, Sulkin MS, Arthur RM, and Efimov IR**. Processing and analysis of cardiac optical mapping data obtained with potentiometric dyes. *Am J Physiol Heart Circ Physiol* 303: H753-765, 2012.

26. **Lee YS, Chang PC, Hsueh CH, Maruyama M, Park HW, Rhee KS, Hsieh YC, Shen C, Weiss JN, Chen Z, Lin SF, and Chen PS**. Apamin-sensitive calcium-activated potassium currents in rabbit ventricles with chronic myocardial infarction. *J Cardiovasc Electrophysiol* 24: 1144-1153, 2013.

27. **Luqman N, Sung RJ, Wang CL, and Kuo CT**. Myocardial ischemia and ventricular fibrillation: pathophysiology and clinical implications. *Int J Cardiol* 119: 283-290, 2007.

28. **Meyer T, Hanson PI, Stryer L, and Schulman H**. Calmodulin trapping by calcium-calmodulin-dependent protein kinase. *Science* 256: 1199-1202, 1992.

29. **Mitsuyama H, Yokoshiki H, Watanabe M, Mizukami K, Shimokawa J, and Tsutsui H**. Ca2+/calmodulin-dependent protein kinase II increases the susceptibility to the arrhythmogenic action potential alternans in spontaneously hypertensive rats. *Am J Physiol Heart Circ Physiol* 307: H199-206, 2014.

30. **Mizukami K, Yokoshiki H, Mitsuyama H, Watanabe M, Tenma T, Takada S, and Tsutsui H**. Small-conductance Ca2+-activated K+ current is upregulated via the phosphorylation of CaMKII in cardiac hypertrophy from spontaneously hypertensive rats. *Am J Physiol Heart Circ Physiol* 309: H1066-1074, 2015.

31. **Nagy N, Szuts V, Horvath Z, Seprenyi G, Farkas AS, Acsai K, Prorok J, Bitay M, Kun A, Pataricza J, Papp JG, Nanasi PP, Varro A, and Toth A**. Does small-conductance calcium-activated potassium channel contribute to cardiac repolarization? *J Mol Cell Cardiol* 47: 656-663, 2009.

32. **Nguyen TP, Sovari AA, Pezhouman A, Iyer S, Cao H, Ko CY, Bapat A, Vahdani N, Ghanim M, Fishbein MC, and Karagueuzian HS**. Increased susceptibility of spontaneously hypertensive rats to ventricular tachyarrhythmias in early hypertension. *J Physiol* 594: 1689-1707, 2016.

33. **Nygren A, Kondo C, Clark RB, and Giles WR**. Voltage-sensitive dye mapping in Langendorff-perfused rat hearts. *Am J Physiol Heart Circ Physiol* 284: H892-902, 2003.

34. **Ozgen N, Dun W, Sosunov EA, Anyukhovsky EP, Hirose M, Duffy HS, Boyden PA, and Rosen MR**. Early electrical remodeling in rabbit pulmonary vein results from trafficking of intracellular SK2 channels to membrane sites. *Cardiovasc Res* 75: 758-769, 2007.

35. **Pezhouman A, Singh N, Song Z, Nivala M, Eskandari A, Cao H, Bapat A, Ko CY, Nguyen TP, Qu Z, Karagueuzian HS, and Weiss JN**. Molecular Basis of

Hypokalemia-Induced Ventricular Fibrillation. *Circulation* 132: 1528-1537, 2015.

36. **Qi XY, Diness JG, Brundel BJ, Zhou XB, Naud P, Wu CT, Huang H, Harada M, Aflaki M, Dobrev D, Grunnet M, and Nattel S**. Role of small-conductance calcium-activated potassium channels in atrial electrophysiology and fibrillation in the dog. *Circulation* 129: 430-440, 2014.

37. **Roeper J, Lorra C, and Pongs O**. Frequency-dependent inactivation of mammalian A-type K+ channel KV1.4 regulated by Ca2+/calmodulin-dependent protein kinase. *J Neurosci* 17: 3379-3391, 1997.

38. **Saito T, Sato T, Miki T, Seino S, and Nakaya H**. Role of ATP-sensitive K+ channels in electrophysiological alterations during myocardial ischemia: a study using Kir6.2-null mice. *Am J Physiol Heart Circ Physiol* 288: H352-357, 2005.

39. **Shimokawa J, Yokoshiki H, and Tsutsui H**. Impaired activation of ATP-sensitive K+ channels in endocardial myocytes from left ventricular hypertrophy. *Am J Physiol Heart Circ Physiol* 293: H3643-3649, 2007.

40. **Sierra A, Zhu Z, Sapay N, Sharotri V, Kline CF, Luczak ED, Subbotina E, Sivaprasadarao A, Snyder PM, Mohler PJ, Anderson ME, Vivaudou M, Zingman LV, and Hodgson-Zingman DM**. Regulation of cardiac ATP-sensitive potassium channel surface expression by calcium/calmodulin-dependent protein kinase II. *J Biol Chem* 288: 1568-1581, 2013.

41. **Uemura A, Naito Y, and Matsubara T**. Dynamics of Ca(2+)/calmodulin-dependent protein kinase II following acute myocardial ischemia-translocation and autophosphorylation. *Biochem Biophys Res Commun* 297: 997-1002, 2002.

42. **Vanheel B, and de Hemptinne A**. Influence of KATP channel modulation on net potassium efflux from ischaemic mammalian cardiac tissue. *Cardiovasc Res* 26: 1030-1039, 1992.

43. **Vittone L, Mundina-Weilenmann C, Said M, Ferrero P, and Mattiazzi A**. Time course and mechanisms of phosphorylation of phospholamban residues in

ischemia-reperfused rat hearts. Dissociation of phospholamban phosphorylation pathways. *J Mol Cell Cardiol* 34: 39-50, 2002.

44. **Wang P, Cao Y, Yu J, Liu R, Bai B, Qi H, Zhang Q, Guo W, Zhu H, and Qu L**. Baicalin alleviates ischemia-induced memory impairment by inhibiting the phosphorylation of CaMKII in hippocampus. *Brain Res* 1642: 95-103, 2016.

45. **Watanabe M, Yokoshiki H, Mitsuyama H, Mizukami K, Ono T, and Tsutsui H**. Conduction and refractory disorders in the diabetic atrium. *Am J Physiol Heart Circ Physiol* 303: H86-95, 2012.

46. **Weston AH, Porter EL, Harno E, and Edwards G**. Impairment of endothelial SK(Ca) channels and of downstream hyperpolarizing pathways in mesenteric arteries from spontaneously hypertensive rats. *Br J Pharmacol* 160: 836-843, 2010.

47. **Wilde AA, Escande D, Schumacher CA, Thuringer D, Mestre M, Fiolet JW, and Janse MJ**. Potassium accumulation in the globally ischemic mammalian heart. A role for the ATP-sensitive potassium channel. *Circ Res* 67: 835-843, 1990.

48. **Xia XM, Fakler B, Rivard A, Wayman G, Johnson-Pais T, Keen JE, Ishii T, Hirschberg B, Bond CT, Lutsenko S, Maylie J, and Adelman JP**. Mechanism of calcium gating in small-conductance calcium-activated potassium channels. *Nature* 395: 503-507, 1998.

49. **Xiao L, Coutu P, Villeneuve LR, Tadevosyan A, Maguy A, Le Bouter S, Allen BG, and Nattel S**. Mechanisms underlying rate-dependent remodeling of transient outward potassium current in canine ventricular myocytes. *Circ Res* 103: 733-742, 2008.

50. **Yokoshiki H, Sunagawa M, Seki T, and Sperelakis N**. ATP-sensitive K+ channels in pancreatic, cardiac, and vascular smooth muscle cells. *Am J Physiol* 274: C25-37, 1998.

51. **Yoo B, Lemaire A, Mangmool S, Wolf MJ, Curcio A, Mao L, and Rockman HA**. Beta1-adrenergic receptors stimulate cardiac contractility and CaMKII activation in vivo and enhance cardiac dysfunction following myocardial infarction. *Am J Physiol Heart Circ Physiol* 297: H1377-1386, 2009.

Figure captions

Figure 1. Study protocol

A, Optical mapping study protocol. **B,** Hypoxic ventricular arrhythmia study protocol. GH, global hypoxia; GH 15, GH 15 min; GH 30, GH 30 min; LV, left ventricle.

Figure 2. Susceptibility to APD abbreviation and SVAs during simulated global hypoxia between WKY rats and SHRs

A, Time course of APD_{90} during global hypoxia (GH) in WKY rats and SHRs. The GH shortened APD_{90} in both WKY (n = 7) and SHR (n = 7). The abbreviation of APD_{90} in SHR occurred earlier than that in WKY. Optical action potentials were recorded at the pacing cycle length (PCL) of 300 ms. **B**, Onset-time of SVAs during GH. The time was earlier in SHRs than in WKY rats, significantly. **C**, Kaplan–Meier curves comparing incidence and time to onset of SVAs from the beginning of GH. The percentage of hearts developing SVAs during GH was higher in SHRs than in WKY rats. $^{*}P < 0.05$, $^{\dagger}P < 0.01$, $^{\ddagger}P < 0.001$, $^{\S}P < 0.0001$. All values are shown as means ± SE. APD, action potential duration; APD_{90}, APD measured at 90% repolarization; B, baseline (GH 0 min); SHR, spontaneous hypertensive rats; SVA, sustained ventricular arrhythmia; WKY, Wistar-Kyoto rats. Other abbreviations are shown in Figure 1.

Figure 3. Electrophysiological and molecular biological changes during acute myocardial hypoxia in WKY rats: Blocking effects of SK channels and K_{ATP} channels.

A and B, Representative changes in optical action potentials (**A**) and APD_{90} maps (**B**) of LV during GH; control (without drug) (CON), with apamin (100 nM) (APA), with glibenclamide (10 μM) (GLB), respectively. Hearts were paced at a cycle length of 300 ms. Optical action potentials were recorded at a black dot in APD_{90} map. A filled triangle in APD_{90} maps is a landmark of the LV apex. **C**, Changes of ΔAPD_{90} in the absence and presence of drugs at GH 15 min (**left**) and GH 30 min (**right**). Apamin reduced APD_{90} abbreviation only at GH 30 min. On the other hand, glibenclamide reduced it at both GH 15 min and GH 30 min. **D,** Representative ECG traces during GH at the pacing cycle length of 300 ms in the absence of drugs (**black line**) and the presence of apamin (100 nM) (**red line**). **E,** Kaplan–Meier curves comparing incidence and time to onset of SVAs from the beginning of GH in the absence and presence drugs. No drugs reduced the incidence of SVAs. **F**, Expression for isoforms of SK channel proteins in left ventricular myocardium during GH (n / N: hearts / animals, 6 / 6 in baseline, 6 / 6 in GH 15 min, 5 / 5 in GH 30 min). GH did not change the amount of any SK channel isoforms. **G**, Expression of Kir 6.2 proteins in left ventricular myocardium during GH (n / N: hearts / animals, 6 / 6 in baseline, 6 / 6 in GH 15 min, 5 / 5 in GH 30 min). The level of Kir 6.2 protein expression was constant during GH. $*P < 0.05$. All values are means ± SE. APA, apamin; CON, control (without drugs); GLB, glibenclamide; n.s., not significant; UCL, UCL-1684. Other abbreviations are shown in Figure 1 and 2.

Figure 4. Electrophysiological and molecular biological changes during acute myocardial hypoxia in SHRs: Blocking effects of SK channels and K_{ATP} channels. **A and B,** Representative changes in optical action potentials (**A**) and APD_{90} maps (**B**) of LV during GH; control (without drug) (CON), with apamin (100 nM) (APA), with glibenclamide (10 μM) (GLB), respectively. Hearts were paced at a cycle length of 300 ms. Optical action potentials were recorded at a black dot in APD_{90} map. A filled triangle in APD_{90} maps is a landmark of the LV apex. **C**, Changes of ΔAPD_{90} in the absence and presence of drugs at GH 15 min (**left**) and GH 30 min (**right**). Apamin reduced APD_{90} abbreviation at both GH 15 min and GH 30 min, significantly. **D,** Representative ECG traces during GH at the pacing cycle length of 300 ms in the absence of drugs (**black line**) and the presence of apamin (100 nM) (**red line**). **E,** Kaplan–Meier curves comparing incidence and time to onset of SVAs from the beginning of GH in the absence and presence drugs. SK channel blockers (apamin, UCL-1684) significantly reduced the incidence of SVAs in SHRs. **F**, Expression for isoforms of SK channel proteins in left ventricular myocardium during GH (n / N: hearts / animals, 6 / 6 in baseline, 6 / 6 in GH 15 min, 5 / 5 in GH 30 min). GH did not change the amount of any SK channel isoforms. **G**, Expression of Kir 6.2 proteins in left ventricular myocardium during GH (n / N: hearts / animals, 6 / 6 in baseline, 6 / 6 in GH 15 min, 5 / 5 in GH 30 min). The level of Kir 6.2 protein expression did not change during GH. $*P < 0.05$. All values are means ± SE. Abbreviations are shown in Figure 1, 2 and 3.

Figure 5. Coefficient of variation of APD in acute myocardial hypoxia

A and B, CV of APD in the absence and presence of drugs at baseline (**left**), GH 15 min (**middle**) and GH 30 min (**right**) in WKY (**A**) and SHR (**B**). There were no significant differences of CV at any hypoxia stage among three groups. All values are means ± SE. Abbreviations are shown in Figure 1, 2 and 3.

Figure 6. Western blot analysis of left ventricular myocardium in WKY rats and SHRs

A, Expression of phosphorylated CaMKII at Thr^{286} (p-CaMKII) in left ventricular myocardium at baseline (state of no GH) (n / N: hearts / animals, 6 / 6 in WKY rats, 6 / 6 in SHRs). Expression of p-CaMKII was higher in SHRs vs. WKY rats at baseline. **B**, Expression of p-CaMKII in left ventricular myocardium during GH from WKY rats (**left**) (n / N: hearts / animals, 6 / 6 in baseline, 6 / 6 in GH 15 min, 6 / 6 in GH 30 min) and SHRs (**right**) (n / N: hearts / animals, 6 / 6 in baseline, 6 / 6 in GH 15 min, 5 / 5 in GH 30 min). In WKY rats, p-CaMKII increased gradually during GH. Otherwise, in SHRs, there were no changes in p-CaMKII expression during GH. **C**, Expression of SK channel isoforms in left ventricular myocardium at baseline (n / N: hearts / animals, 6 / 6 in WKY rats, 6 / 6 in SHRs). Only SK2 channel proteins were higher in SHRs. **D**, Expression of Kir 6.2 in left ventricular myocardium at baseline (n / N: hearts / animals, 6 / 6 in WKY rats, 6 / 6 in SHRs). There was no difference with regard to Kir 6.2 protein expression between WKY rats and SHRs. $^{*}P < 0.05$. All values are expressed as means ± SE. n = 5 - 6 for each group. Abbreviations are shown in Figure 1, 2 and 3.

Figure 7. Interaction of p-CaMKII and SK channels in left ventricular myocardium from SHR.

A. Immunoprecipitation was performed with the anti-p-CaMKII antibodies and probed for the isoform of SK channel proteins by western blot with the anti-SK1(**upper**), SK2 (**middle**), and SK3 (**lower**) antibodies. **B**. Immunoprecipitation was performed with the anti-SK1(**upper**), SK2 (**middle**), and SK3 (**lower**) antibodies, and probed for p-CaMKII by western blot with the anti-p-CaMKII antibodies. Only SK2 channel protein interacted with p-CaMKII. IB, immunoblotting; IP, immunoprecipitation.

Figure 8. Proposed mechanisms of the altered SK channel activity in normal and hypertrophied hearts during acute myocardial hypoxia.

At baseline (state of no hypoxia), the sensitivity of SK channels to Ca^{2+} are different between normal and hypertrophied hearts. This may be because the p-CaMKII bound SK channel in cardiac hypertrophy has a high Ca^{2+} sensitivity. **A,** At the early phase of hypoxia, SK channels in a hypertrophied heart, but not in a normal heart, are activated, thereby contributing to the abbreviation of APD because of high Ca^{2+} sensitivity. **B,** At the delayed phase of hypoxia, in hypertrophied heart, SK channel activation is unchanged: SK channels have still high activity, and SK channels in normal heart are also activated by elevation of intracellular Ca^{2+} and subsequent increase in p-CaMKII. The increased p-CaMKII binds to SK channels, thereby being more sensitive to Ca^{2+}.

Figure 1

A

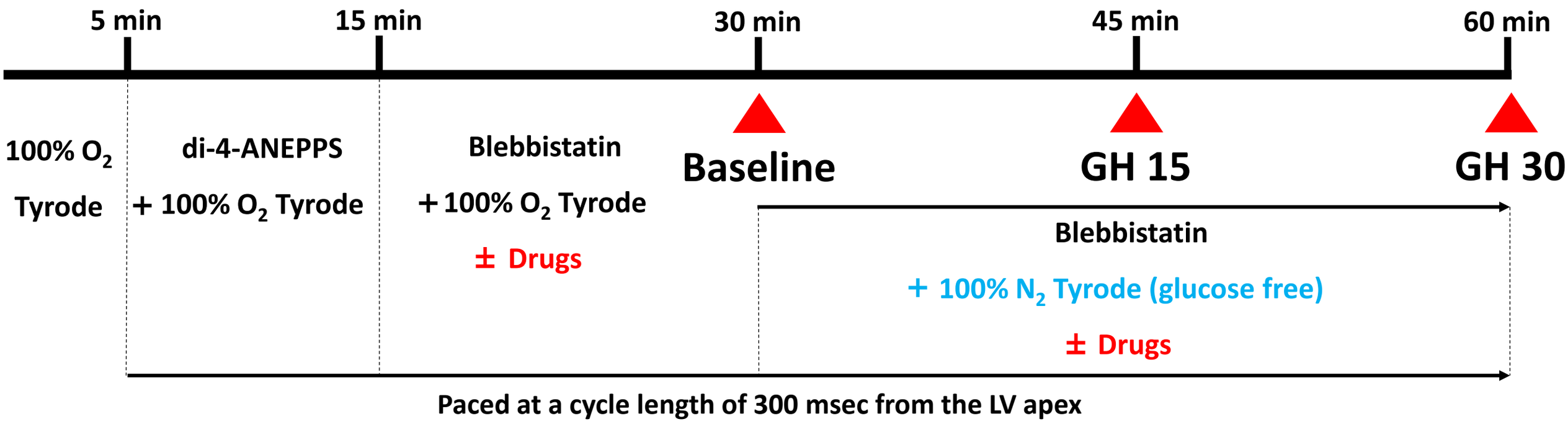

▲ Optical data acquisition point

B

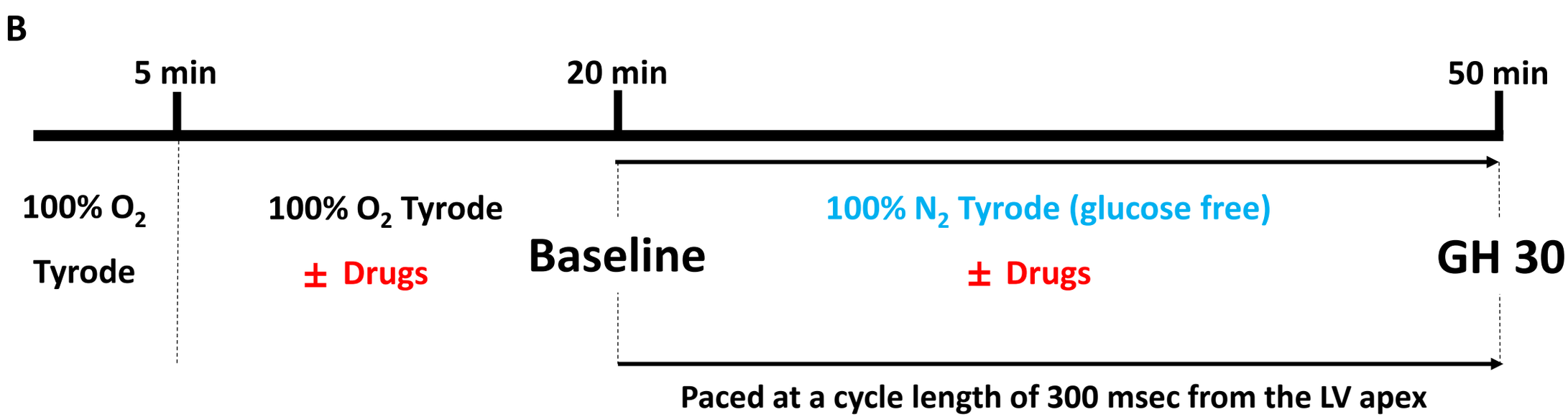

Figure 2

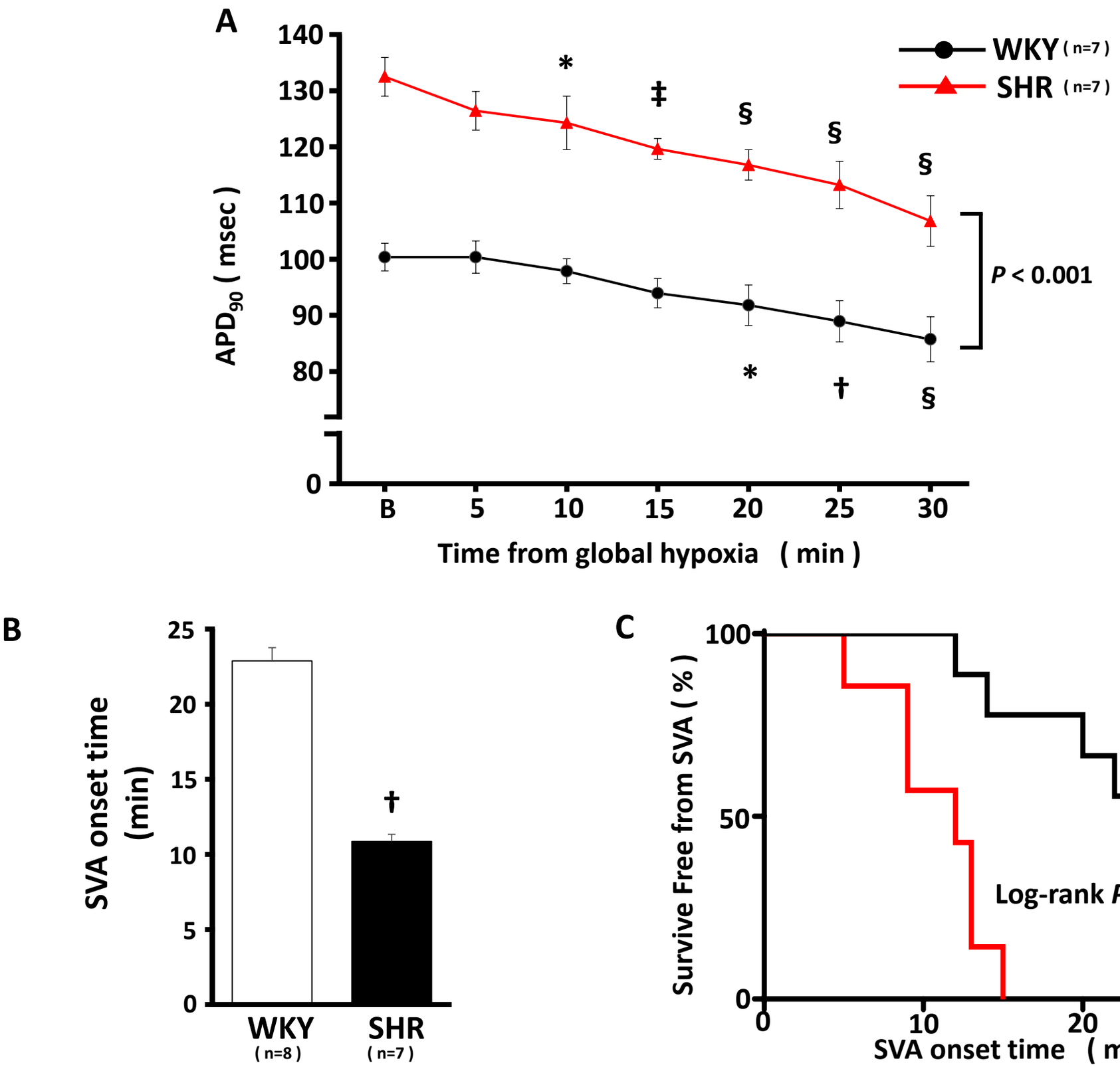
A
140
130
120
110
100
90
80
0
APD90 (msec)
*
‡
§
§
§
*
†
§
WKY (n=7)
SHR (n=7)
P < 0.001
B
25
20
15
10
5
0
SVA onset time (min)
†
WKY (n=8)
SHR (n=7)
C
100
50
0
Survive Free from SVA (%)
WKY (n=9)
SHR (n=7)
Log-rank P < 0.01
0
10
20
30
SVA onset time (min)
B
5
10
15
20
25
30
Time from global hypoxia (min)

Figure 3

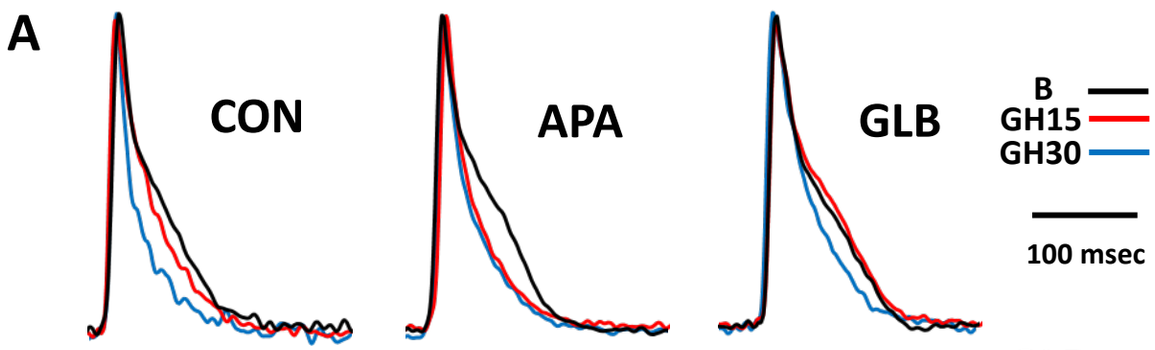
A
CON
APA
GLB
B
GH15
GH30
100 msec

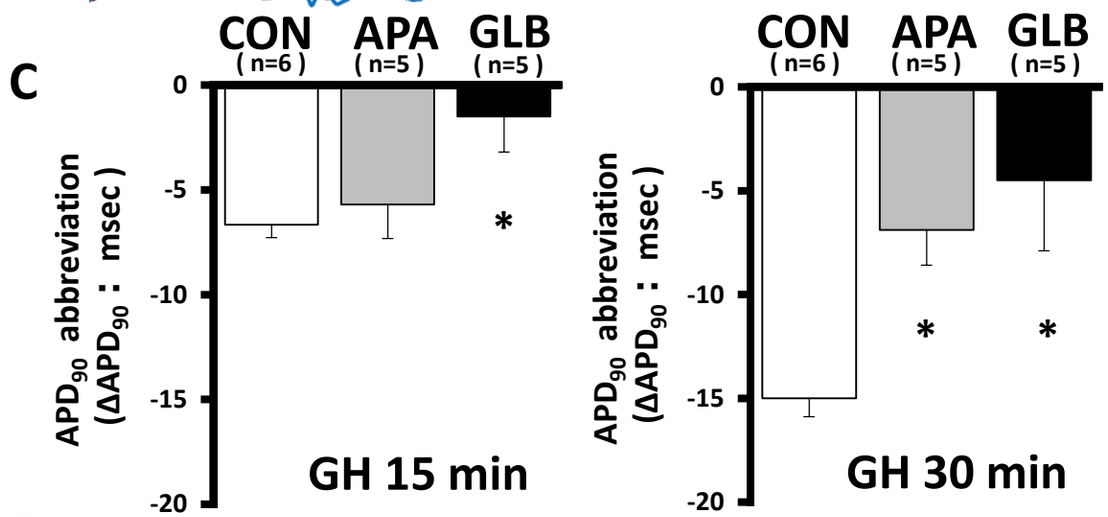
C
CON
APA
GLB
(n=6)
(n=5)
(n=5)
APD90 abbreviation (ΔAPD90 : msec)
0
-5
-10
-15
-20
*
GH 15 min
GH 30 min

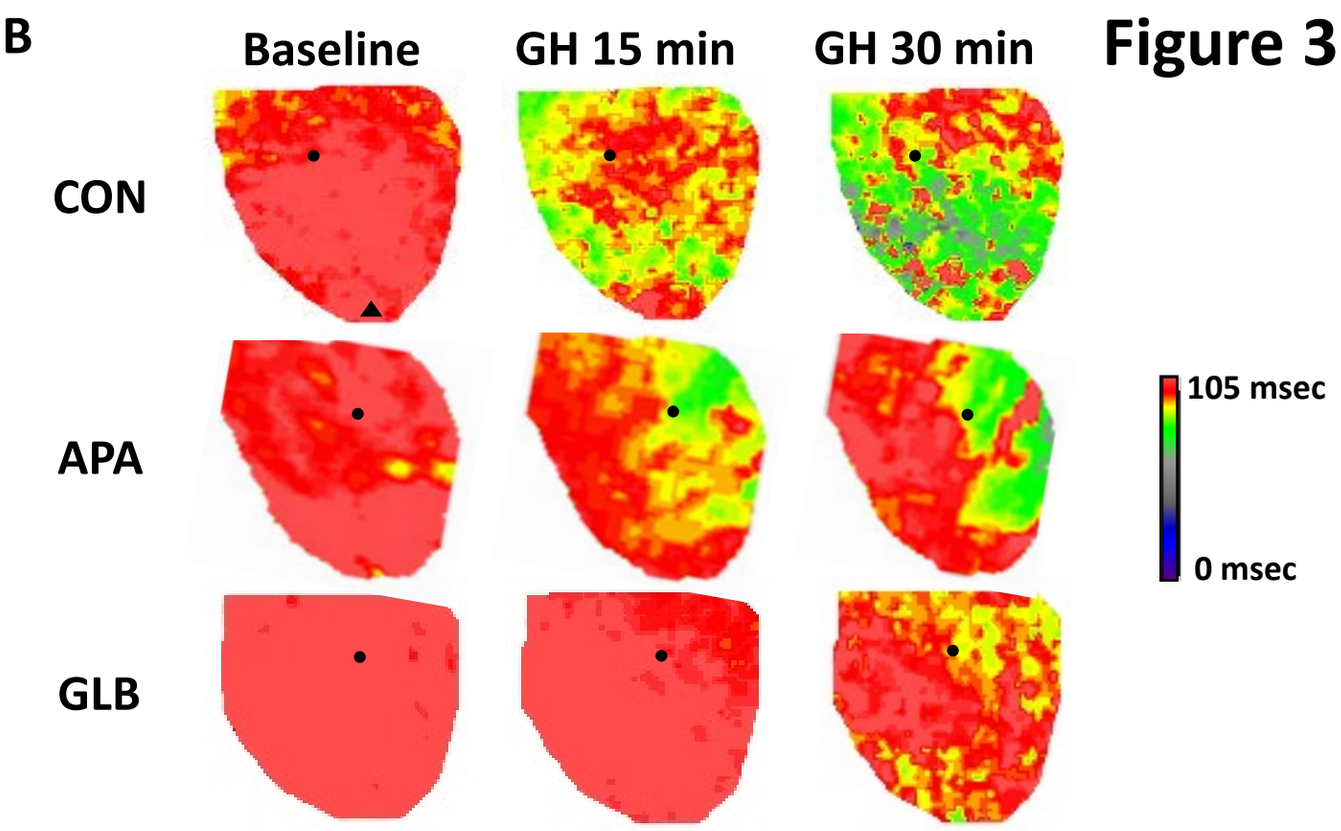
B
Baseline
GH 15 min
GH 30 min
CON
APA
GLB
105 msec
0 msec

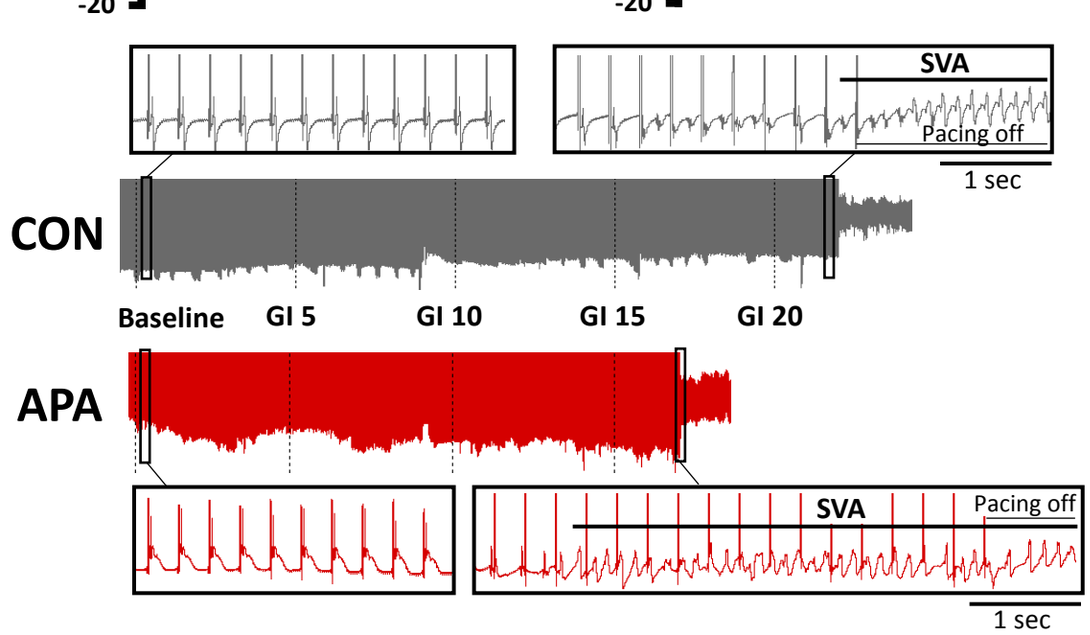
D
SVA
Pacing off
1 sec
CON
Baseline
GI 5
GI 10
GI 15
GI 20
APA
SVA
Pacing off
1 sec

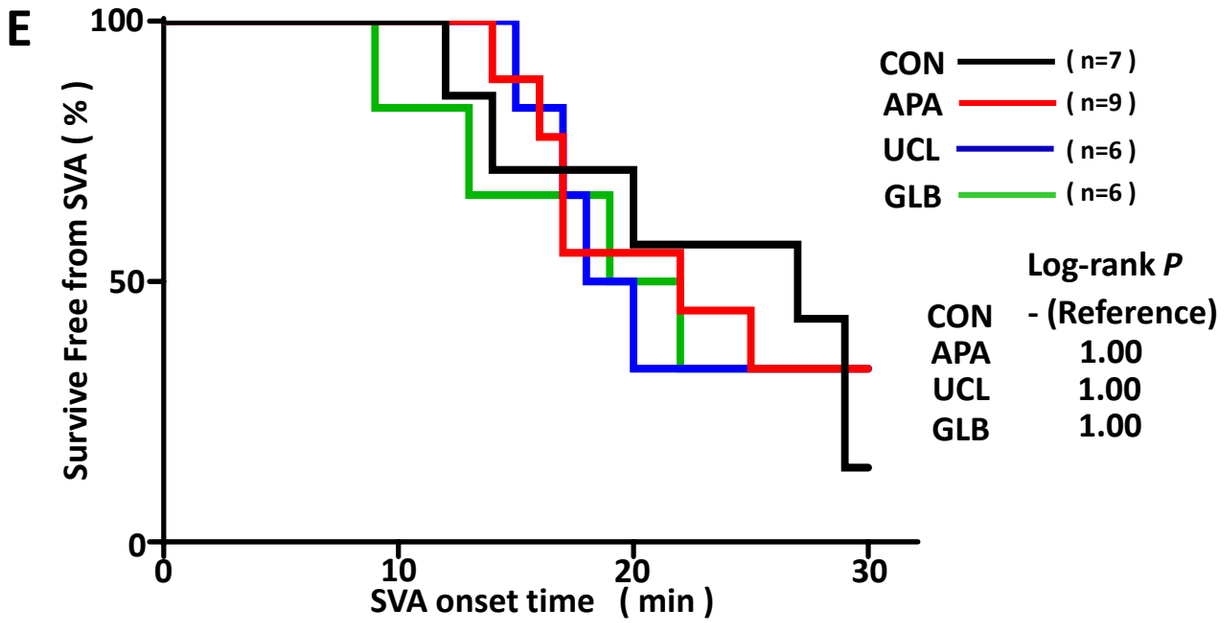
E
100
50
0
Survive Free from SVA (%)
0
10
20
30
SVA onset time (min)
CON (n=7)
APA (n=9)
UCL (n=6)
GLB (n=6)
Log-rank P
CON - (Reference)
APA 1.00
UCL 1.00
GLB 1.00

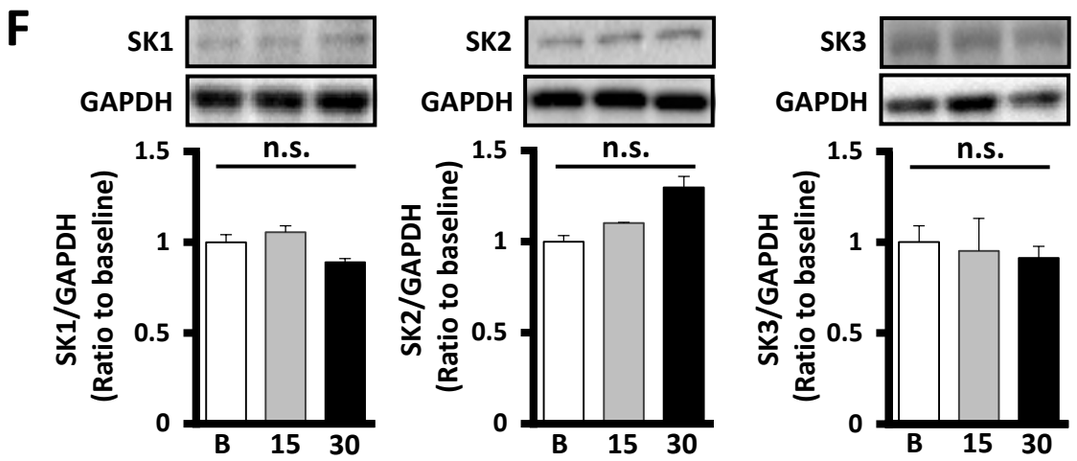
F
SK1
SK2
SK3
GAPDH
n.s.
SK1/GAPDH (Ratio to baseline)
SK2/GAPDH (Ratio to baseline)
SK3/GAPDH (Ratio to baseline)
1.5
1
0.5
0
B
15
30

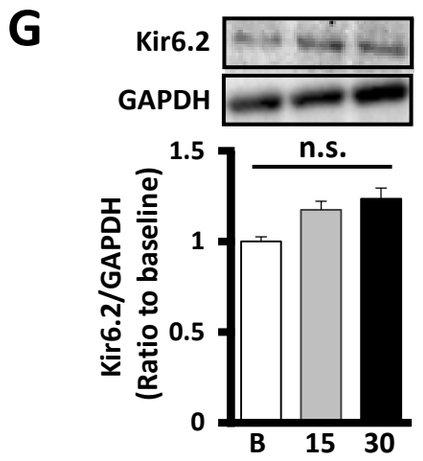
G
Kir6.2
GAPDH
n.s.
Kir6.2/GAPDH (Ratio to baseline)
1.5
1
0.5
0
B
15
30

Figure 4

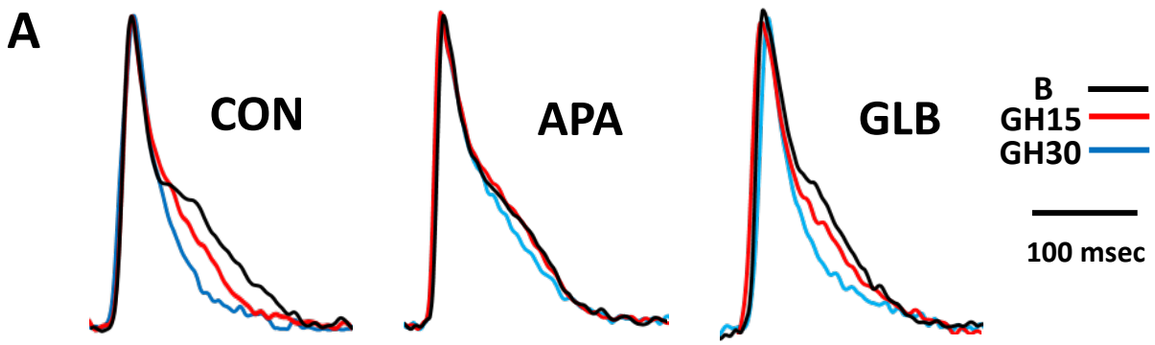
A
CON
APA
GLB
B
GH15
GH30
100 msec

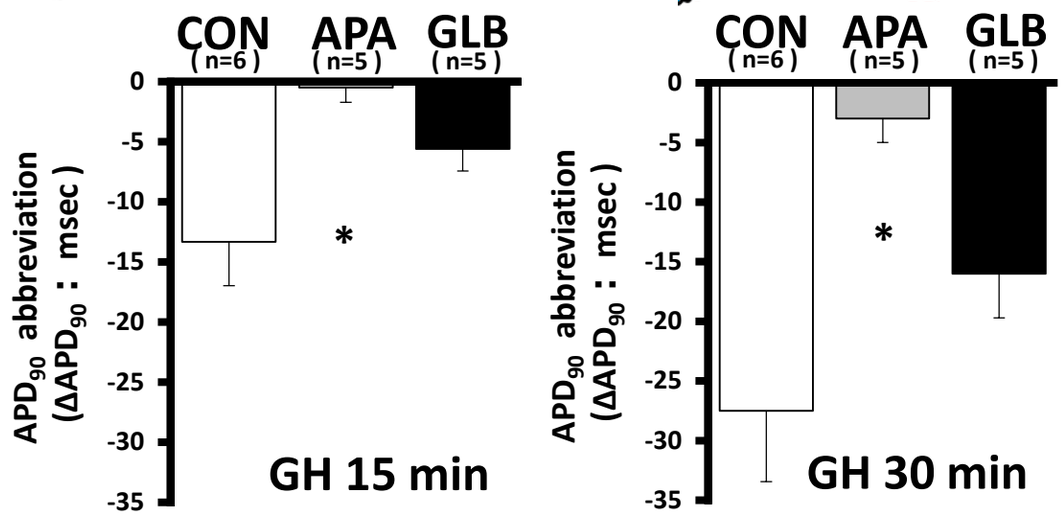
C
CON
APA
GLB
(n=6)
(n=5)
(n=5)
APD90 abbreviation (ΔAPD90 : msec)
0
-5
-10
-15
-20
-25
-30
-35
*
GH 15 min
GH 30 min

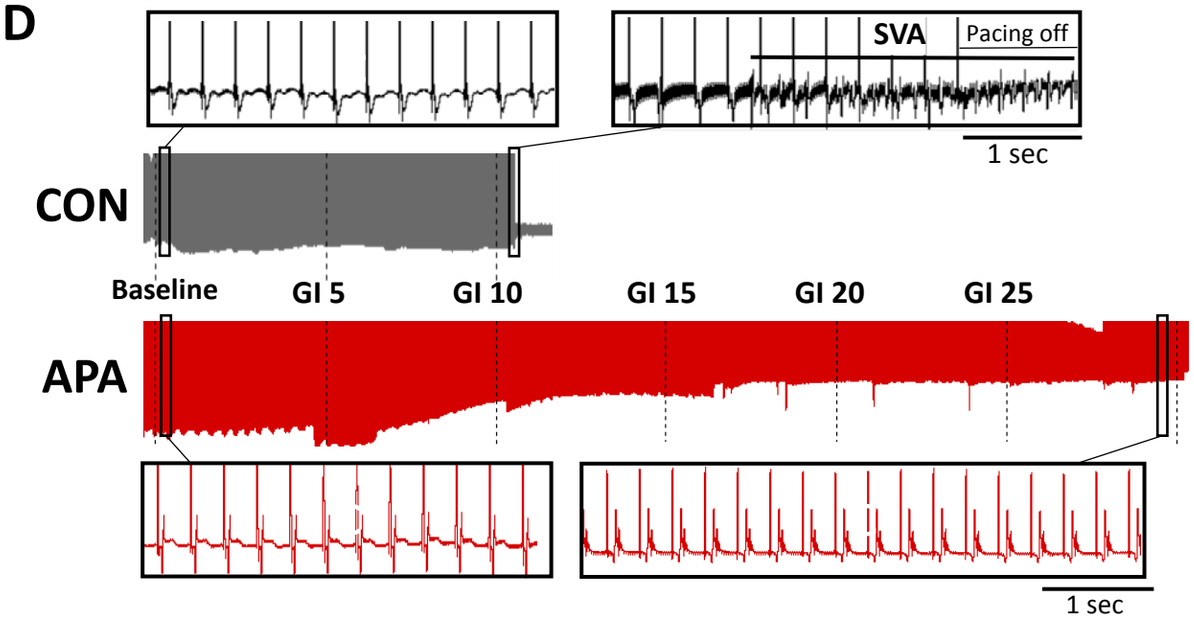
D
SVA
Pacing off
1 sec
CON
Baseline
GI 5
GI 10
GI 15
GI 20
GI 25
APA
1 sec

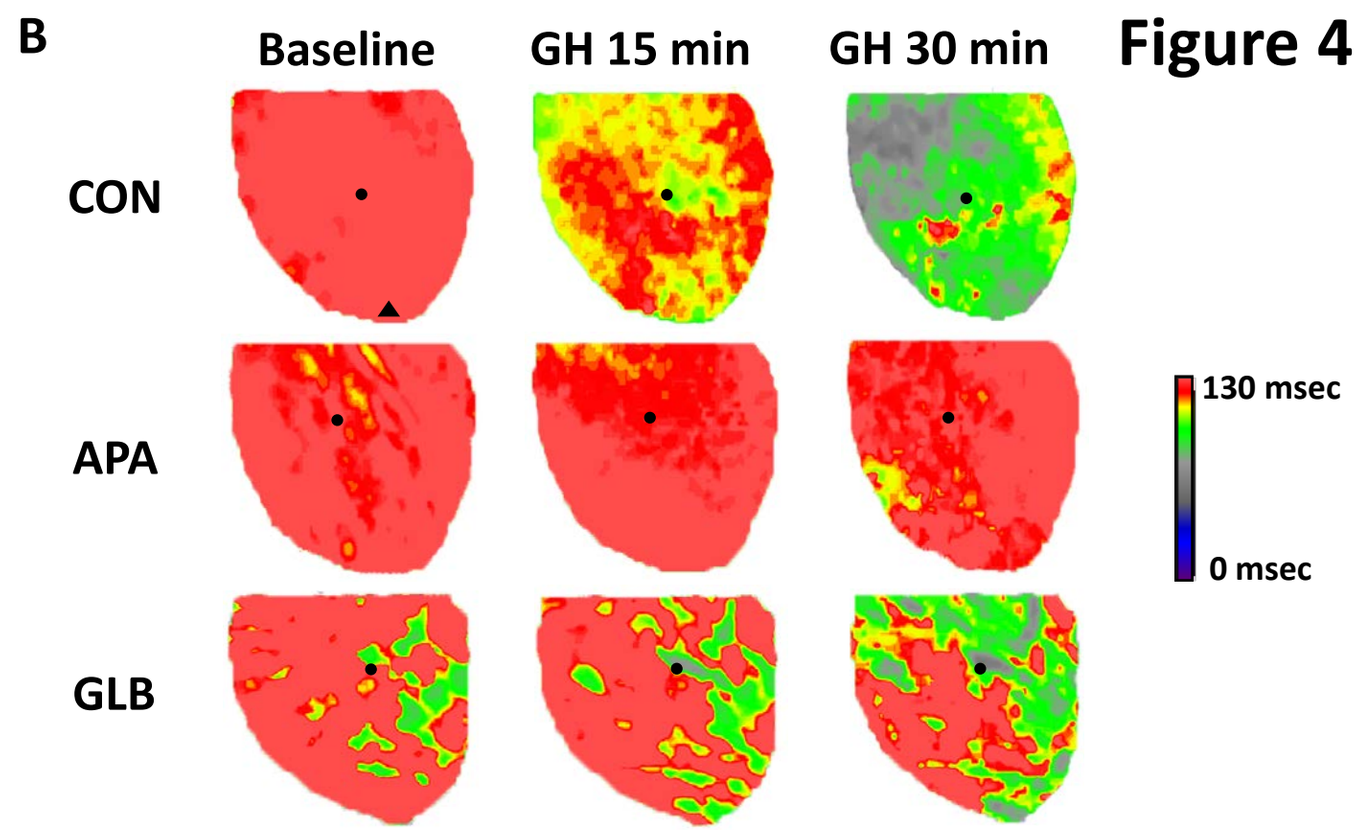
B
Baseline
GH 15 min
GH 30 min
CON
APA
GLB
130 msec
0 msec

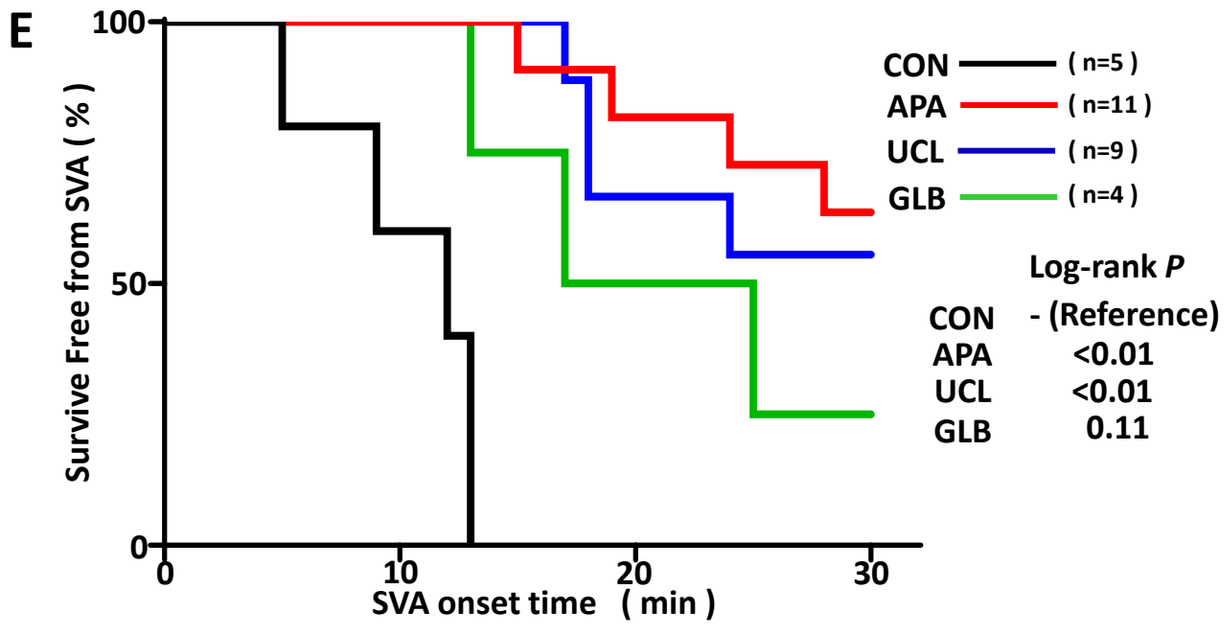
E
Survive Free from SVA (%)
100
50
0
0
10
20
30
SVA onset time (min)
CON (n=5)
APA (n=11)
UCL (n=9)
GLB (n=4)
Log-rank P
CON - (Reference)
APA <0.01
UCL <0.01
GLB 0.11

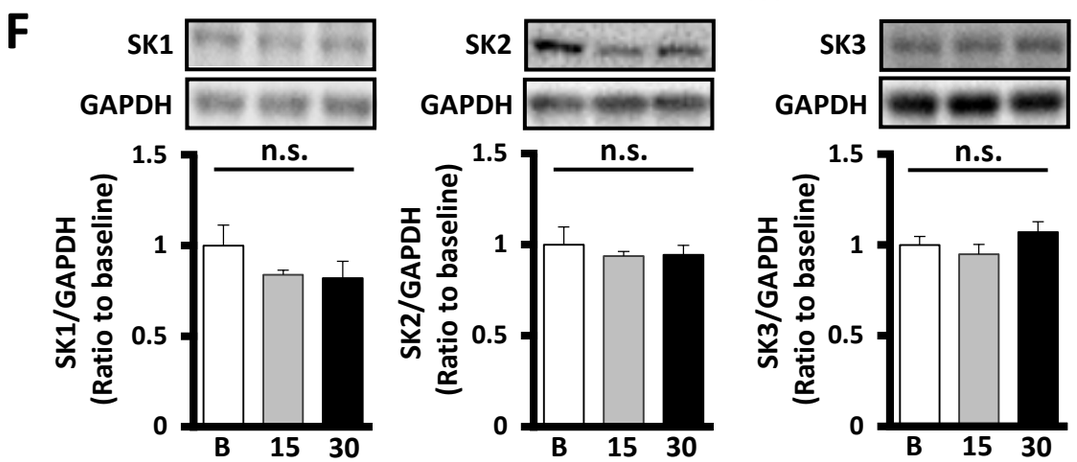
F
SK1
GAPDH
SK2
GAPDH
SK3
GAPDH
n.s.
SK1/GAPDH (Ratio to baseline)
SK2/GAPDH (Ratio to baseline)
SK3/GAPDH (Ratio to baseline)
1.5
1
0.5
0
B
15
30

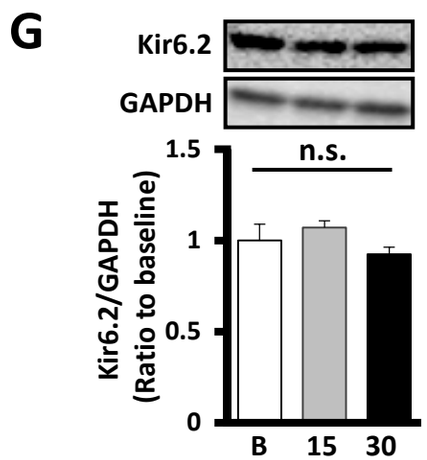
G
Kir6.2
GAPDH
n.s.
Kir6.2/GAPDH (Ratio to baseline)
1.5
1
0.5
0
B
15
30

Figure 5

A

WKY

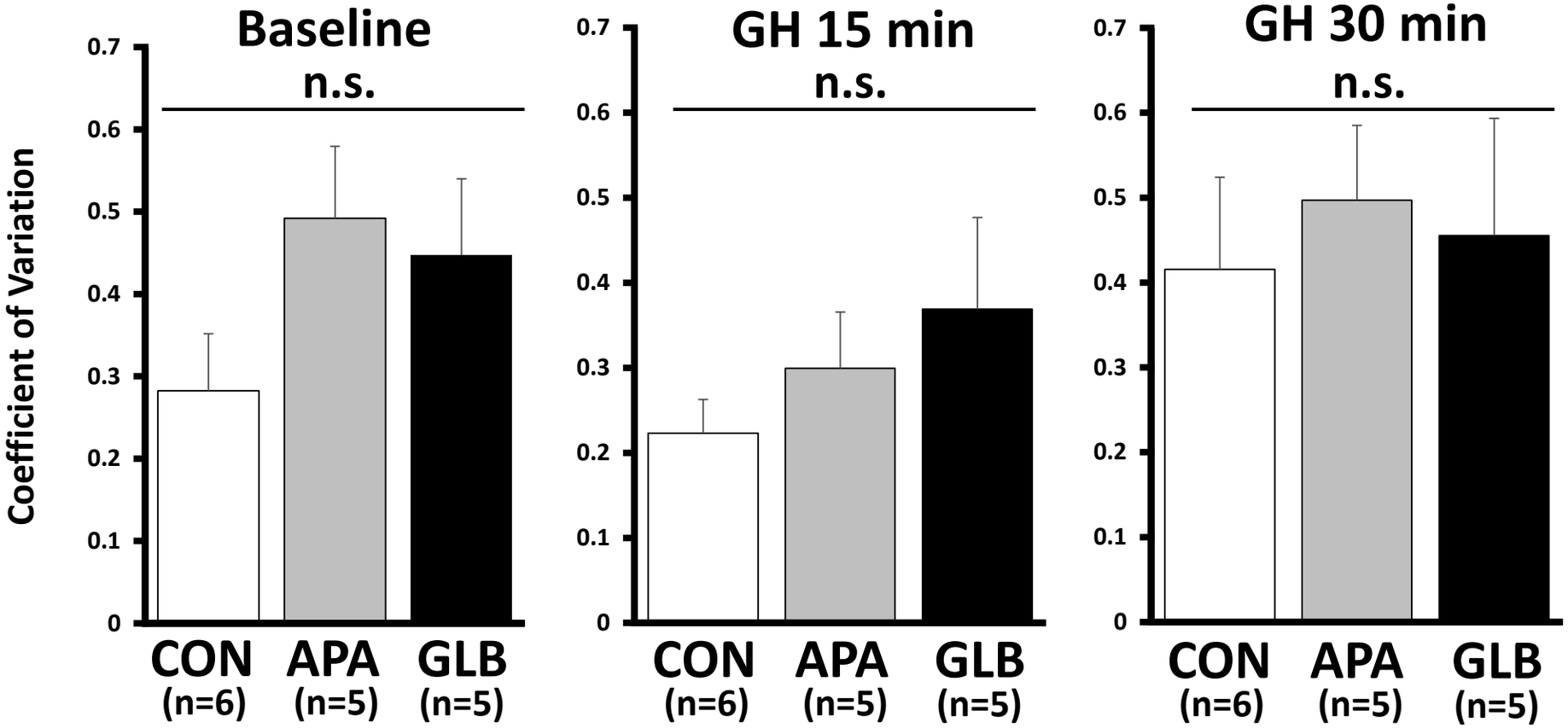

B

SHR

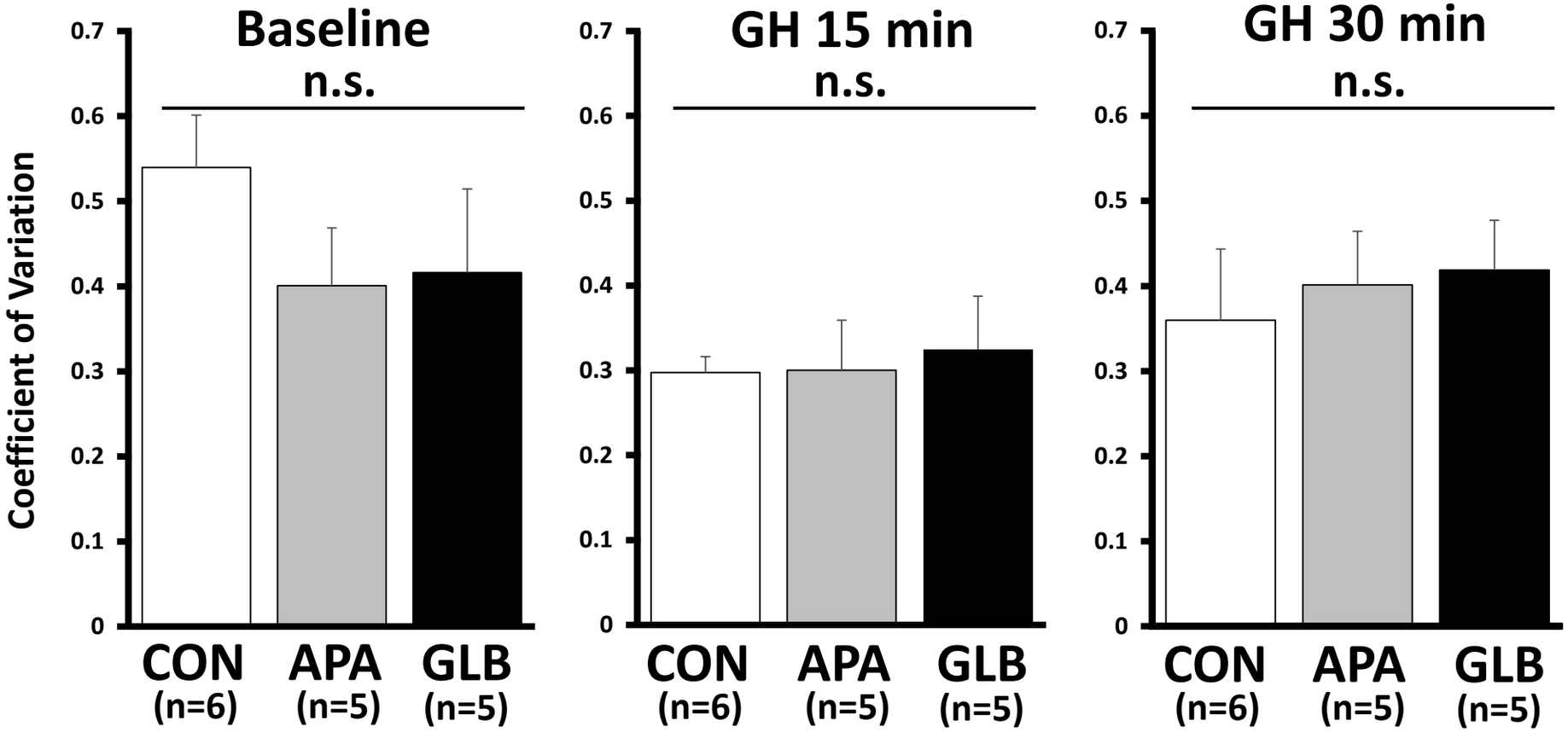

Figure 6

A

Baseline

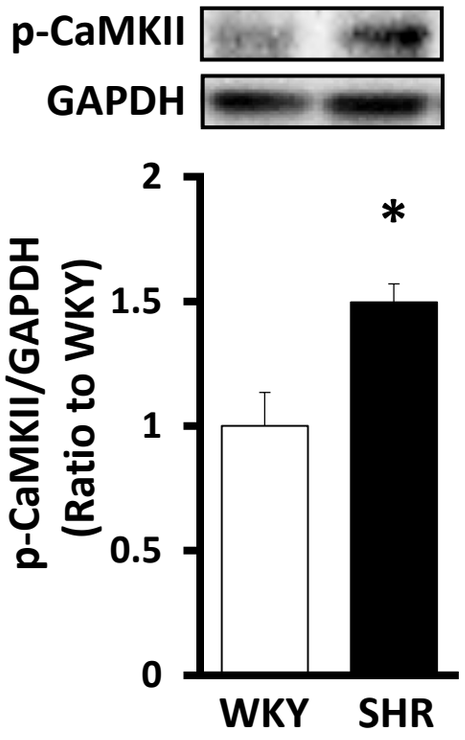

B

WKY

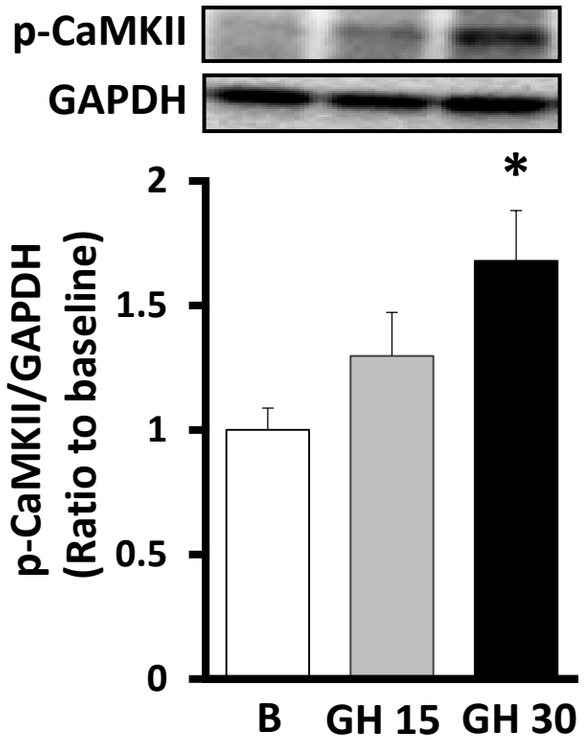

SHR

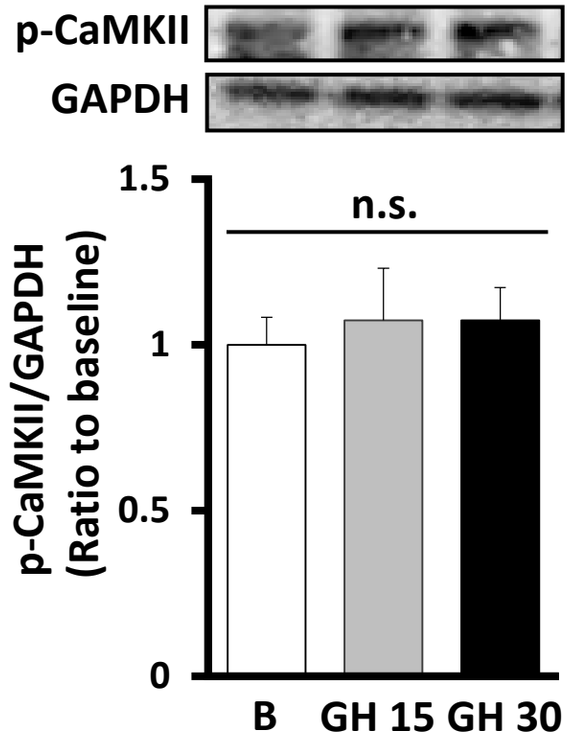

C

Baseline

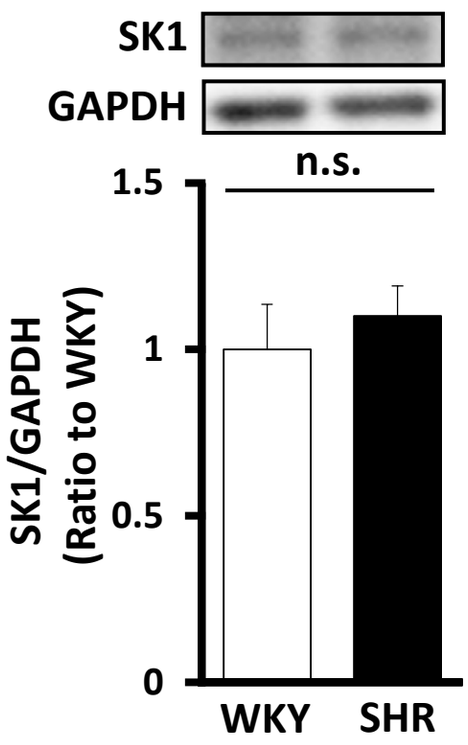

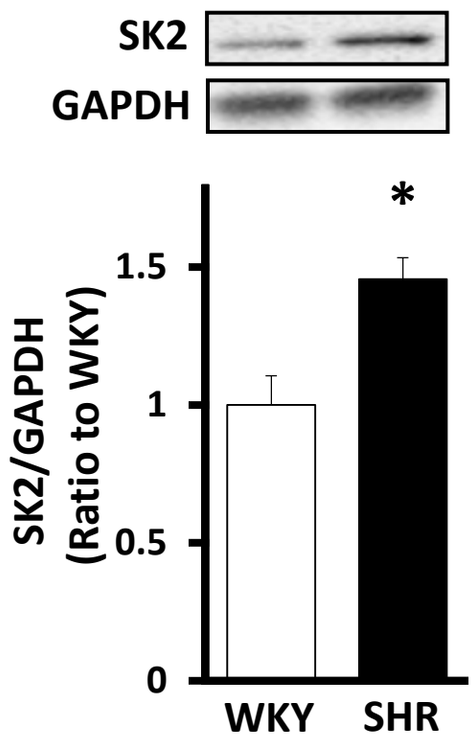

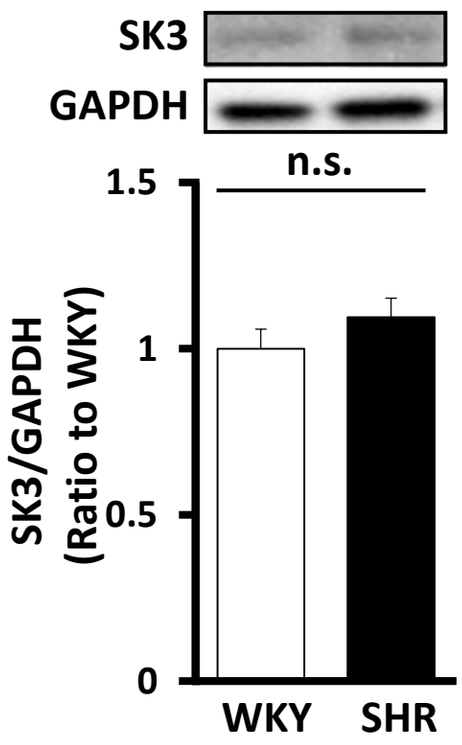

D

Baseline

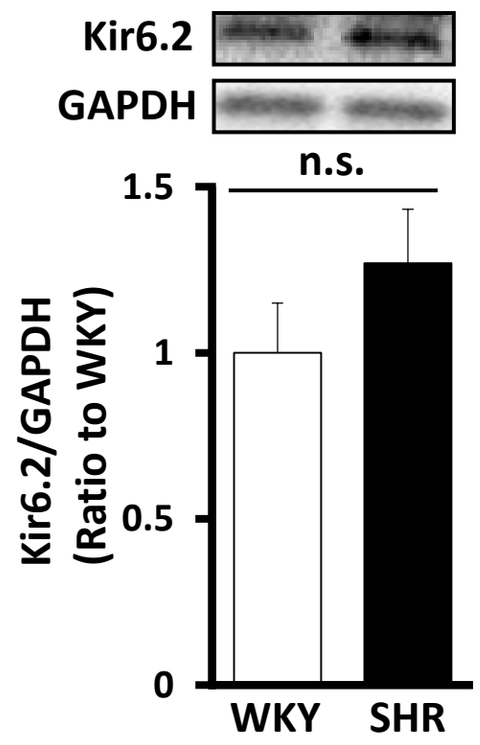

Figure 7

A

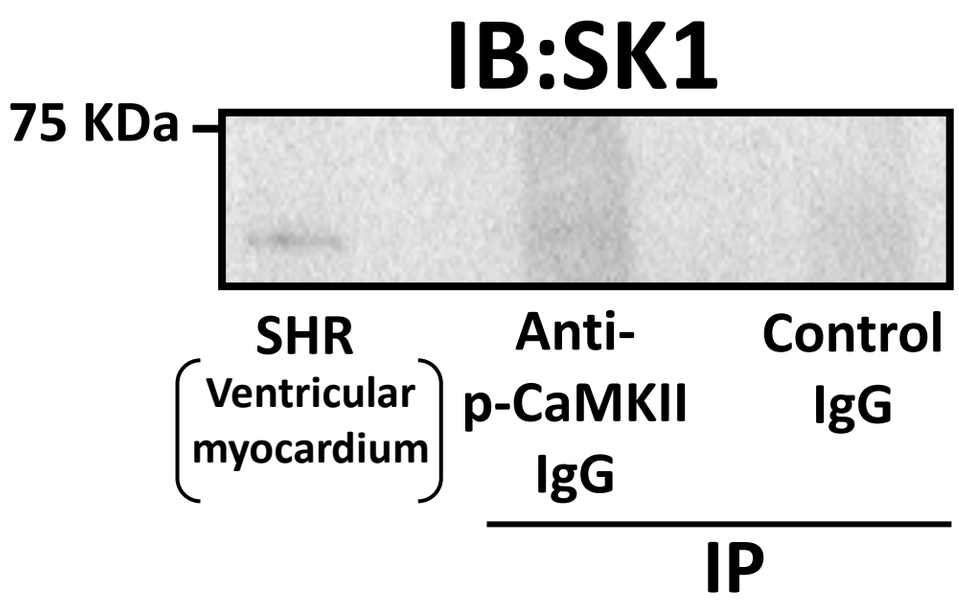
IB:SK1
75 KDa
SHR
Ventricular myocardium
Anti-p-CaMKII IgG
Control IgG
IP
IB:SK2
75 KDa
SHR
Ventricular myocardium
Anti-p-CaMKII IgG
Control IgG
IP
IB:SK3
75 KDa
SHR
Ventricular myocardium
Anti-p-CaMKII IgG
Control IgG
IP

B

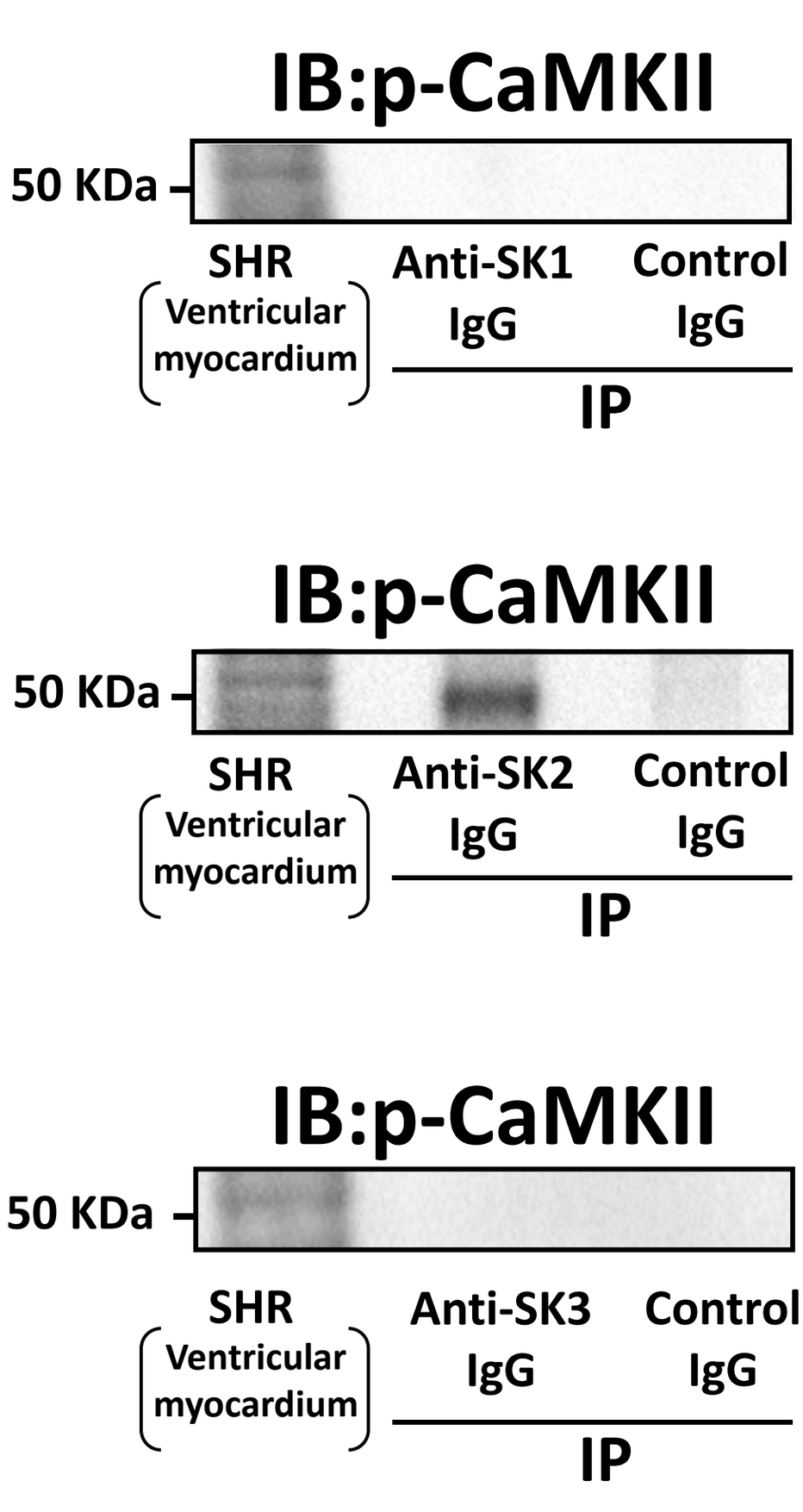
IB:p-CaMKII
50 KDa
SHR
Ventricular myocardium
Anti-SK1 IgG
Control IgG
IP
IB:p-CaMKII
50 KDa
SHR
Ventricular myocardium
Anti-SK2 IgG
Control IgG
IP
IB:p-CaMKII
50 KDa
SHR
Ventricular myocardium
Anti-SK3 IgG
Control IgG
IP

Figure 8

A

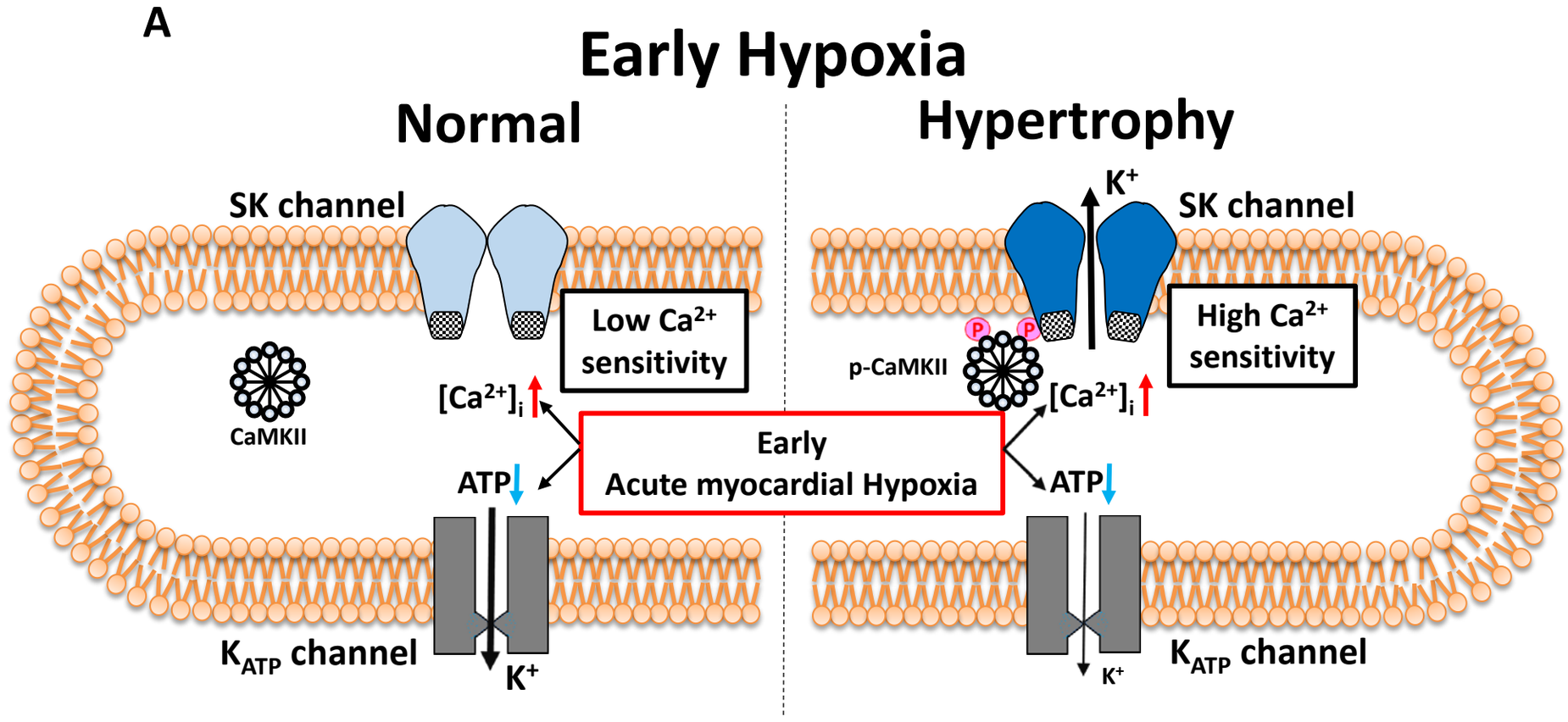
Early Hypoxia
Normal
Hypertrophy
SK channel
Low Ca2+ sensitivity
CaMKII
[Ca2+]i
ATP
Early
Acute myocardial Hypoxia
KATP channel
K+
K+
SK channel
High Ca2+ sensitivity
p-CaMKII
P
P
[Ca2+]i
ATP
KATP channel
K+

B

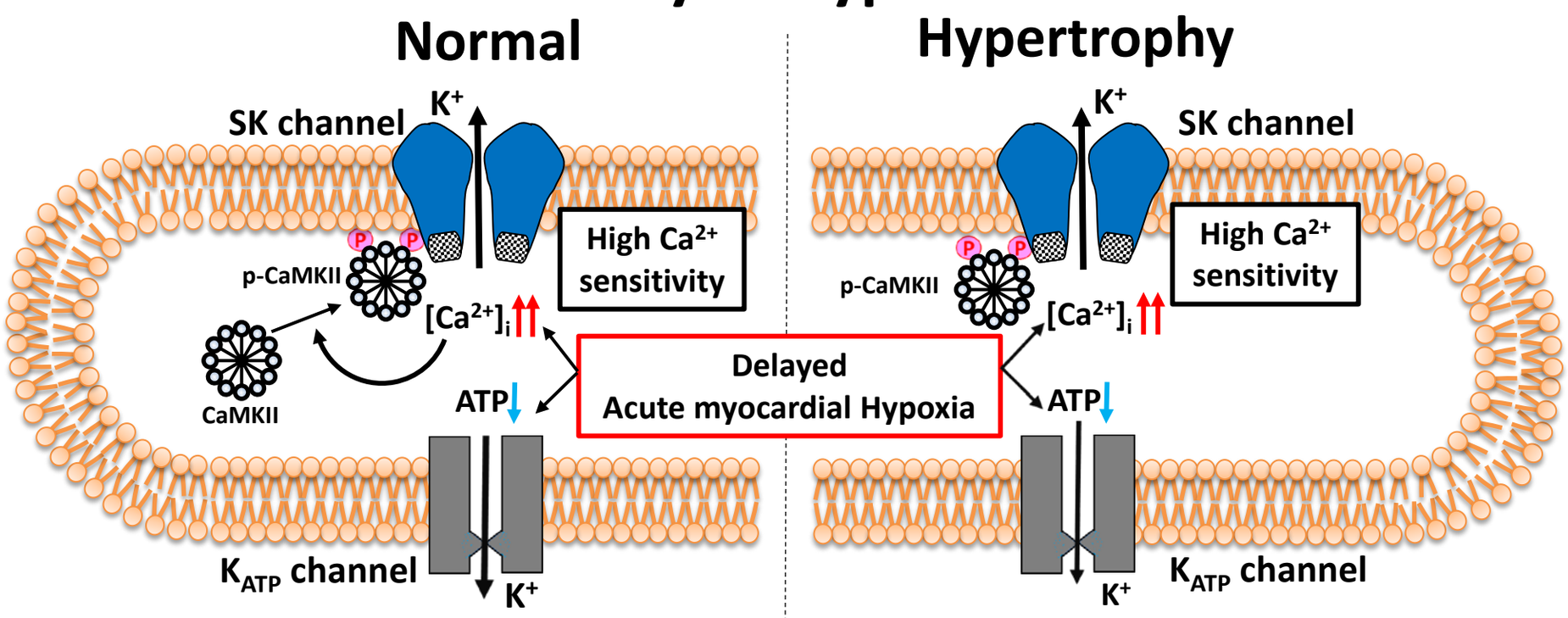
Delayed Hypoxia
Normal
Hypertrophy
SK channel
K+
High Ca2+ sensitivity
p-CaMKII
P
P
CaMKII
[Ca2+]i
ATP
Delayed
Acute myocardial Hypoxia
KATP channel
K+
K+
SK channel
High Ca2+ sensitivity
p-CaMKII
[Ca2+]i
ATP
KATP channel
K+